

# Fractional magnetization plateaux of a spin-1/2 Heisenberg model on the Shastry-Sutherland lattice: effect of quantum XY interdimer coupling

T. Verkholyak<sup>1\*</sup>, J. Strečka<sup>2</sup>

<sup>1</sup> Institute for Condensed Matter Physics, NASU, 1 Svientsitskii Street, Lviv-11, 79011, Ukraine

<sup>2</sup> Department of Theoretical Physics and Astrophysics, Faculty of Science, P. J. Šafárik University, Park Angelinum 9, 040 01, Košice, Slovakia

\* werch@icmp.lviv.ua

April 16, 2021

## Abstract

Spin-1/2 Heisenberg model on the Shastry-Sutherland lattice is considered within the many-body perturbation theory developed from the exactly solved spin-1/2 Ising-Heisenberg model with the Heisenberg intradimer and Ising interdimer interactions. The former model is widely used for a description of magnetic properties of the layered compound  $\text{SrCu}_2(\text{BO}_3)_2$ , which exhibits a series of fractional magnetization plateaux at sufficiently low temperatures. Using the novel type of many-body perturbation theory we have found the effective model of interacting triplet excitations with the extended hard-core repulsion, which accurately recovers 1/8, 1/6 and 1/4 magnetization plateaux for moderate values of the interdimer coupling. A possible existence of a striking quantum phase of bound triplons with a stripe-like character of bound-triplon waves is also revealed at low enough magnetic fields.

---

## Contents

1	Introduction	2
2	Shastry-Sutherland model	3
3	Effective model of triplon excitations	6
4	Quantum correlated phase of bound triplons	12
5	Conclusions	15
A	Diagonalization of the Ising-Heisenberg model	16
B	Technical details of the perturbation theory	18
	References	25

## 1 Introduction

The spin-1/2 quantum Heisenberg model on the Shastry-Sutherland lattice [1], which is traditionally referred to as the Shastry-Sutherland model, is the modern playground for the study of the complex structure of quantum matter emergent in low-dimensional spin systems. Its structure is characterized by the two-dimensional array of mutually orthogonal spin dimers [2]. The competition between the antiferromagnetic intradimer  $J$  and interdimer  $J'$  couplings brings on the shortly-correlated singlet-dimer and singlet-plaquette phases in the ground state [1, 3]. The application of the magnetic field invokes several subtle fractional magnetization plateaux with complex ordering of localized triplon excitations (see Ref. [4] for a review). The theoretical study of the Shastry-Sutherland model generally represents a complex problem tackled by many numerical methods like CORE [5], pCUTs [6–8], tensor network iPEPS [9–11], and others (for a review see Ref. [2]). Besides, the possible emergence of bound states [9, 12–16], topological triplon modes [17, 18] and Bose-Einstein condensation [2, 19] is of the current research interest. Recently, the numerical variational approach shed light on the quantum phases emerging at the boundary of the singlet-dimer phase [20]. The study of thermodynamics is even more complex due to a problem with thermal averaging. Most recently the QMC method has been specifically adapted to the Shastry-Sutherland model in a dimer basis in order to avoid a sign problem within QMC simulations of this frustrated quantum spin system [21, 22]. Temperature-driven phase transitions are being another challenging task, which nowadays attract considerable attention [23–25].

The most prominent experimental representative of the Shastry-Sutherland model is the layered magnetic material  $\text{SrCu}_2(\text{BO}_3)_2$ . Being rediscovered by Kageyama *et al.* [26], this magnetic compound provides a long sought after experimental realization of the singlet-dimer phase at zero magnetic field and several exotic quantum phases, which are manifested in a low-temperature magnetization curve as a series of fractional magnetization plateaux [10, 27]. What is even more, the ratio between the intradimer and interdimer couplings in this magnetic compound is quite close to a phase boundary between the singlet-dimer phase and the singlet-plaquette phase [3]. It turns out that the external pressure indeed paves the way for tuning the relative ratio between the interdimer and intradimer coupling constants through the crystal deformation and hence, one may observe at low enough temperatures a phase transition between the singlet-dimer, singlet-plaquette and Néel phases [28]. Physical manifestations of these phases in  $\text{SrCu}_2(\text{BO}_3)_2$  is under intense current experimental and theoretical research [29–33]. Nevertheless, even the magnetic behavior at low magnetic fields is still not completely understood yet. In Ref. [27] the fractional magnetization plateaux at  $1/8$ ,  $2/15$ ,  $1/6$ ,  $1/4$  of the saturation magnetization were revealed by nuclear magnetic resonance and torque measurements at  $T = 60$  mK, while in Ref. [10] magnetization measurements at ultrahigh magnetic fields gave evidence for the  $1/8$ ,  $1/4$ ,  $1/3$ ,  $1/2$  magnetization plateaux recorded at  $T = 2.4$  K.

It should be noted that  $\text{SrCu}_2(\text{BO}_3)_2$  is not the only example of the physical realization of the Shastry-Sutherland model. The magnetic structure of  $(\text{CuCl})\text{Ca}_2\text{Nb}_3\text{O}_{10}$  is also consistent with the Shastry-Sutherland model, but the ferromagnetic character of the interdimer cou-

pling regrettably prevents emergence of fractional plateaus in the respective low-temperature magnetization curves [34,35]. On the other hand, the rare-earth tetraborides  $RB_4$  ( $R = Dy, Er, Tm, Tb, Ho$ ) afford another intriguing class of the magnetic materials, which display a complex structure of fractional magnetization plateaus inherent to the anisotropic Heisenberg model on the Shastry-Sutherland lattice with a rather strong Ising-type anisotropy [36–42]. While the antiferromagnetic spin-1/2 Ising model on the Shastry-Sutherland lattice is capable of reproducing the fractional 1/3-plateau only [43], the possible spin-electron coupling in the metallic rare-earth tetraborides may be essential for a description of their magnetic properties [44,45].

In the present work we will consider the Shastry-Sutherland model by means of the strong-coupling approach based on the perturbative treatment of  $XY$  interdimer interaction. In Sec. 2 we will define the model and expose the applied perturbative method. In Sec. 3 we will discuss in particular the results of the second-order perturbation theory with the main emphasis laid on the phases of localized triplons emergent in the ground-state phase diagram. Here, we will also demonstrate to what extent the sequence of the fractional plateaux in  $SrCu_2(BO_3)_2$  can be described. The quantum correlated phases are considered in Sec. 4, while the most interesting findings are summarized in Sec. 5. Some specific technical details of the calculation procedure are shown in Appendices.

## 2 Shastry-Sutherland model

Let us consider the spin-1/2 Heisenberg model on the Shastry-Sutherland lattice [1] in an external magnetic field defined by the following Hamiltonian:

$$H = J \sum_{\langle l,m \rangle} \mathbf{s}_l \cdot \mathbf{s}_l + J' \sum_{\langle\langle l,m \rangle\rangle} \mathbf{s}_l \cdot \mathbf{s}_m - h \sum_l s_l^z, \quad (1)$$

where  $\langle l, m \rangle$  and  $\langle\langle l, m \rangle\rangle$  denote the summation over all intradimer  $J$  and interdimer  $J'$  interactions, the general site index  $l = (n, i, j)$  involves a reference number  $n = 1$  or  $2$  of the spin in a dimer in addition to two reference numbers  $i$  and  $j$  specifying the dimer's position in a column and a row of the Shastry-Sutherland lattice, respectively (see Fig. 1 for enumeration of sites). Last, the parameter  $h = g\mu_B H$  denotes the standard Zeeman's term,  $\mu_B$  is the Bohr magneton,  $g$  is the gyromagnetic factor of magnetic ions and  $H$  is the external magnetic field.

A usual procedure for the perturbative treatment starts from the limit of non-interacting dimers leaving the weaker interdimer coupling as a perturbation [14,46]. However, such an approach is slowly converging and requires the higher-order expansion terms. For instance, the expansion up to third order is able to reproduce only the 1/2 and 1/3 plateaux of the Shastry-Sutherland model [14]. In the present work we will develop the unconventional perturbation theory from the exact solution for the ground state of the spin-1/2 Ising-Heisenberg model on the Shastry-Sutherland lattice with the Heisenberg intradimer and Ising interdimer couplings given by the Hamiltonian [47]:

$$H_{IH} = J \sum_{\langle l,m \rangle} \mathbf{s}_l \cdot \mathbf{s}_m + J' \sum_{\langle\langle l,m \rangle\rangle} s_l^z s_m^z - h \sum_l s_l^z. \quad (2)$$

If the intradimer interaction is assumed to be much stronger than the interdimer interaction, i.e.  $J > J'$ , it is convenient to utilize the dimer-state basis for a pair of spins coupled by the

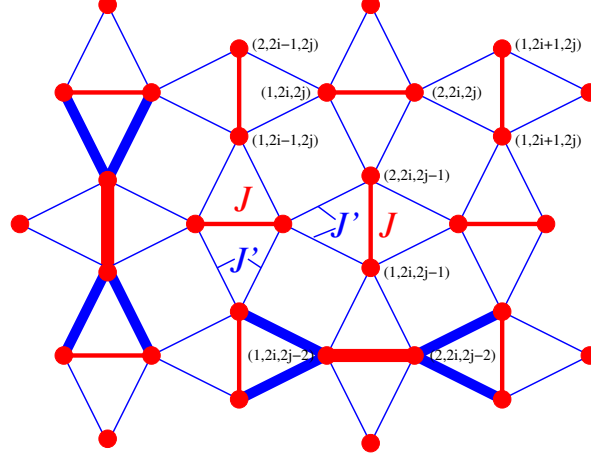


Figure 1: A schematic representation of the Shastry-Sutherland model defined through the Hamiltonian (1). Thick (red) lines denote the stronger intradimer coupling  $J$ , while thin (blue) lines show the interdimer coupling  $J'$ . Bold lines mark clusters of three subsequent strongly correlated dimers in the Ising-Heisenberg model given by the Hamiltonian (2).

stronger intradimer interaction:

$$\begin{aligned}
 |0\rangle_{i,j} &= \frac{1}{\sqrt{2}}(|\uparrow\rangle_{1,i,j}|\downarrow\rangle_{2,i,j} - |\downarrow\rangle_{1,i,j}|\uparrow\rangle_{2,i,j}), \\
 |1\rangle_{i,j} &= |\uparrow\rangle_{1,i,j}|\uparrow\rangle_{2,i,j}, \\
 |2\rangle_{i,j} &= \frac{1}{\sqrt{2}}(|\uparrow\rangle_{1,i,j}|\downarrow\rangle_{2,i,j} + |\downarrow\rangle_{1,i,j}|\uparrow\rangle_{2,i,j}), \\
 |3\rangle_{i,j} &= |\downarrow\rangle_{1,i,j}|\downarrow\rangle_{2,i,j},
 \end{aligned} \tag{3}$$

where  $|0\rangle_{i,j}$  denotes the singlet-dimer state, and  $|1\rangle_{i,j}$ ,  $|2\rangle_{i,j}$ ,  $|3\rangle_{i,j}$  correspond to the triplet-dimer state with the following values of  $z$ -component of the total spin  $S_{i,j}^z = s_{1,i,j}^z + s_{2,i,j}^z = 1, 0, -1$ , respectively. Such a representation provides a transparent description of all ground states, which emerge in the spin-1/2 Ising-Heisenberg model on the Shastry-Sutherland lattice given by the Hamiltonian (2) [47]. In fact, the  $z$ -component of the total spin on a dimer  $S_{i,j}^z$  is a well defined quantum number and the Hamiltonian  $H_{IH}$  can be brought into a diagonal form by the unitary transformation (see Ref. [47] and Appendix A for further details). Thus, the problem of finding its ground state is turned into the minimization of the diagonalized Hamiltonian with respect to the quantum states on local dimers. It has been verified previously [47] that the ground state of the spin-1/2 Ising-Heisenberg model on the Shastry-Sutherland lattice (2) for  $J' \leq J$  can be characterized by the following four phases: the singlet-dimer phase for  $h < h_{c1}$ , the stripe 1/3-plateau phase (see Fig. 2) for  $h_{c1} < h < h_{c2}$ , the checkerboard 1/2-plateau phase for  $h_{c2} < h < h_{c3}$  and the saturated paramagnetic phase for  $h > h_{c3}$ . The critical fields determining the relevant ground-state phase boundaries are explicitly given as

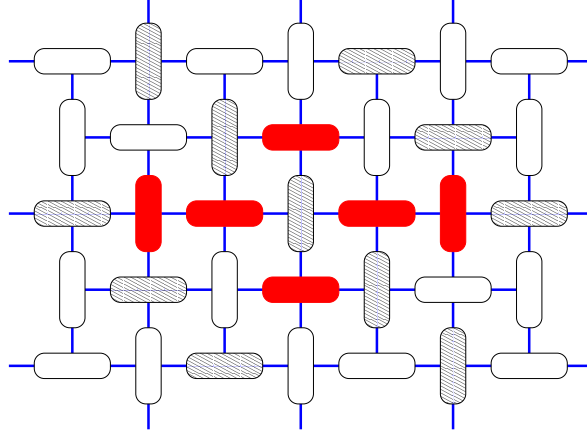


Figure 2: The schematic representation of the stripe  $1/3$ -plateau phase and a hard-core repulsion condition for triplons. Dashed (empty) rounded rectangle denote  $S^z = 1$  triplet (singlet) states on dimers. The dimers marked in red exemplify a hard-core constraint for a central dimer in a triplet state, which excludes triplons on all its four nearest-neighbor dimers as well as two alike oriented further-neighbor dimers along one spatial direction.

follows:

$$\begin{aligned}
 h_{c1} &= 2J - \sqrt{J^2 + J'^2}, \\
 h_{c2} &= -J + 2\sqrt{J^2 + J'^2}, \\
 h_{c3} &= J + 2J'.
 \end{aligned} \tag{4}$$

It should be pointed out that the ground state of the spin-1/2 Ising-Heisenberg model on the Shastry-Sutherland lattice is macroscopically degenerate at the first critical field  $h_{c1}$  and moreover, this highly degenerate ground-state manifold can be treated as a gas of  $S^z = 1$  triplet excitations referred to as triplons [48] emergent on a background of the crystal of singlet dimers. It has been shown previously [47] that the ground states of the spin-1/2 Ising-Heisenberg model on the Shastry-Sutherland lattice can be constructed from a six-spin cluster composed of three consecutive dimers (see Fig. 1) under the following restriction: no more than one triplon excitation can be located on each six-spin cluster. Consequently, such triplet excitations should obey the hard-core constraint: triplons cannot be created on four adjacent (nearest-neighbor) dimers and such an exclusion rule should be additionally extended for a vertically (horizontally) oriented dimer to its two alike oriented further-neighbor dimers in horizontal (vertical) direction (see Fig. 2).

In the following our attention will be focused on a phase boundary between the singlet-dimer and stripe  $1/3$ -plateau phases, i.e. the magnetic-field region sufficiently close to the first critical field  $h_{c1}$ , where the low-temperature magnetization curve of the spin-1/2 Heisenberg model on the Shastry-Sutherland lattice exhibits the most spectacular features (see Ref. [4] for a review). To this end, the Hamiltonian (2) of the spin-1/2 Ising-Heisenberg model on the Shastry-Sutherland lattice at the critical field  $h = h_{c1}$  with exactly known ground state will be considered as an unperturbed part of the Hamiltonian (1) of the spin-1/2 Heisenberg model on the Shastry-Sutherland lattice, whereas the remaining part of the Hamiltonian (1)

involving the  $XY$ -part of the interdimer interaction will be perturbatively treated together with the deviation of the magnetic field from the critical value  $h_{c1}$ :

$$H' = J' \sum_{\langle\langle l,m \rangle\rangle} (s_l^x s_m^x + s_l^y s_m^y) - (h - h_{c1}) \sum_l s_l^z. \quad (5)$$

It should be noted that the feasibility of the perturbation method might be limited at very small values of the interaction ratio  $J'/J$  due to the fact that the energy of the configuration with two triplons placed on adjacent dimers is quite close to the ground state.

### 3 Effective model of triplon excitations

Let us apply the many-body perturbation theory (see for instance Ref. [49] for a general procedure) to the  $XY$ -part of the interdimer interaction at the phase boundary between the singlet-dimer and stripe 1/3-plateau phase, where the ground state is macroscopically degenerate and can be presented as a lattice gas of triplet excitations on dimers. Within the second-order perturbation expansion one obtains the following effective Hamiltonian when excluding from consideration two triplet states  $|2\rangle_{i,j}$ ,  $|3\rangle_{i,j}$  of each dimer while retaining only the singlet state  $|0\rangle_{i,j}$  and fully polarized triplet state  $|1\rangle_{i,j}$  (see Appendix B for details):

$$\begin{aligned} H_{eff} &= \mathcal{P}_0 [E_0 + H_1 + H_t + H_2 + H_3 + \dots] \mathcal{P}_0, \\ H_1 &= (e_0 + h_{c1} - h) \sum_{\mathbf{l}} n_{\mathbf{l}}, \quad \mathbf{l} = (l_x, l_y), \\ H_2 &= V_1 \sum_{\langle\langle l,l' \rangle\rangle} n_{\mathbf{l}} n_{\mathbf{l}'} + V_2 \sum_{\langle\langle l,l' \rangle\rangle'} n_{\mathbf{l}} n_{\mathbf{l}'} + V_3 \sum_{\langle\langle l,l' \rangle\rangle''} n_{\mathbf{l}} n_{\mathbf{l}'}, \\ H_3 &= V_{\Delta 1} \sum_{\langle\langle l,l',l'' \rangle\rangle_1} n_{\mathbf{l}} n_{\mathbf{l}'} n_{\mathbf{l}''} + V'_{\Delta 1} \sum_{\langle\langle l,l',l'' \rangle\rangle'_1} n_{\mathbf{l}} n_{\mathbf{l}'} n_{\mathbf{l}''} + V_{\Delta 2} \sum_{\langle\langle l,l',l'' \rangle\rangle_2} n_{\mathbf{l}} n_{\mathbf{l}'} n_{\mathbf{l}''} \\ &\quad + V'_{\Delta 2} \sum_{\langle\langle l,l',l'' \rangle\rangle'_2} n_{\mathbf{l}} n_{\mathbf{l}'} n_{\mathbf{l}''} + V''_{\Delta 2} \sum_{\langle\langle l,l',l'' \rangle\rangle''_2} n_{\mathbf{l}} n_{\mathbf{l}'} n_{\mathbf{l}''} + V_{\Delta 3} \sum_{\langle\langle l,l',l'' \rangle\rangle_3} n_{\mathbf{l}} n_{\mathbf{l}'} n_{\mathbf{l}''}, \\ H_t &= t \sum'_{i,j=1}^N (n_{i,j-1} + n_{i,j+1}) (a_{i-1,j}^+ a_{i+1,j} + a_{i-1,j} a_{i+1,j}^+) \\ &\quad + t \sum''_{i,j=1}^N (n_{i-1,j} + n_{i+1,j}) (a_{i,j-1}^+ a_{i,j+1} + a_{i,j-1} a_{i,j+1}^+). \end{aligned} \quad (6)$$

The summation symbol  $\sum'$  ( $\sum''$ ) is restricted by the constraint  $i + j = \text{odd}$  ( $i + j = \text{even}$ ) extended over all vertical (horizontal) dimers and  $\mathcal{P}_0$  is the projection operator incorporating the hard-core condition for triplons (see Fig. 2 and Eq. (19)). Each site of the effective model (6) corresponds to a dimer of the Shastry-Sutherland lattice, and an empty (filled) site  $n_{\mathbf{l}} = 0$  ( $n_{\mathbf{l}} = 1$ ) of the effective model is assigned to the singlet state  $|0\rangle_{\mathbf{l}}$  (triplet state  $|1\rangle_{\mathbf{l}}$ ) of the  $l$ th dimer of the original Shastry-Sutherland model (1). In addition to the occupation number operator  $n_{\mathbf{l}}$  we have also introduced the creation and annihilation hard-core boson operators  $a_{\mathbf{l}}^+$  and  $a_{\mathbf{l}}$ , which describe the transformation of the  $l$ th dimer from the singlet state  $|0\rangle_{\mathbf{l}}$  to the triplet state  $|1\rangle_{\mathbf{l}}$  and vice versa. The physical meaning of individual terms entering into the

effective Hamiltonian (6) are as follows:  $H_1$  corresponds to the renormalized energy of a single triplon,  $H_2$  describes effective pair interactions between triplons placed on further-neighbor dimers (see Fig. 3),  $H_3$  contains the most valuable contributions among effective three-particle interactions between triplons (see Fig. 4), and  $H_t$  represents the correlated hopping term (see Fig. 5).

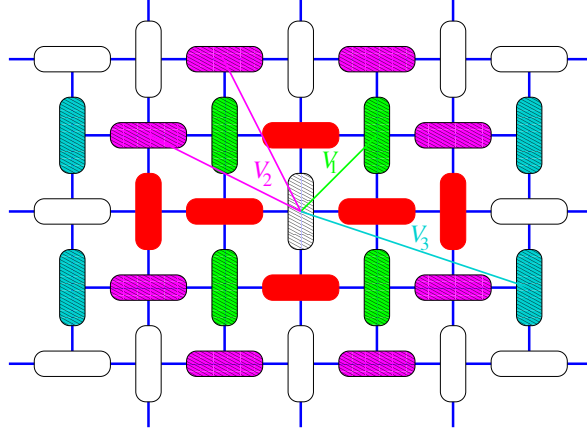


Figure 3: A schematic representation of effective pair interactions between triplons. Red rounded rectangles around the central dimer in the triplet state (dashed rounded rectangle) shows the hard-core condition, the colored rectangles indicate the interaction between the central triplon and its further neighbors.

Up to the second-order expansion, there are no direct tunneling terms for triplons. It should be mentioned, however, that such terms are negligibly small also in the ordinary strong-coupling approach starting from noninteracting dimers, where they appear only in the 6th order of the perturbation expansion [50]. Besides, the complete effective Hamiltonian developed up to the second order would also contain effective many-body interactions of higher order (e.g. four-, five-, six-particle couplings), but their contributions are negligibly small in comparison with the effective pair and three-particle interactions. Hence, the higher-order effective interactions do not have any essential impact and we have therefore left out all those terms from the effective Hamiltonian (6). For completeness, the coupling constants with a significant impact on a magnetic behavior entering in the effective Hamiltonian (6) are explicitly given in Appendix B, whereas their respective dependencies on a relative size of the coupling constants  $J'/J$  are shown in Fig. 6. In general, the magnitude of the effective couplings are relatively small for all values of the coupling ratio  $J'/J$ , which stabilize the singlet-dimer phase at zero magnetic field. Note furthermore that the three effective pair interactions generally decay with distance between dimers. Surprisingly, the correlated hopping parameter prevails at sufficiently small values of the interaction ratio  $J'/J$ , while the effective pair interaction  $V_1$  between closest-spaced triplons allowed by the hard-core constraint (Fig. 2 and Eq. (19)) becomes the most dominant at higher values of the coupling ratio  $J'/J$ . It is evident from a comparison of Fig. 6(a) and (b) that the effective three-particle couplings are much smaller in magnitude than the effective pair interactions and thus, they do not have an essential impact on phase boundaries between different ground states. Moreover, the strength of the effective three-particle couplings drops off rapidly with the distance between triplons.

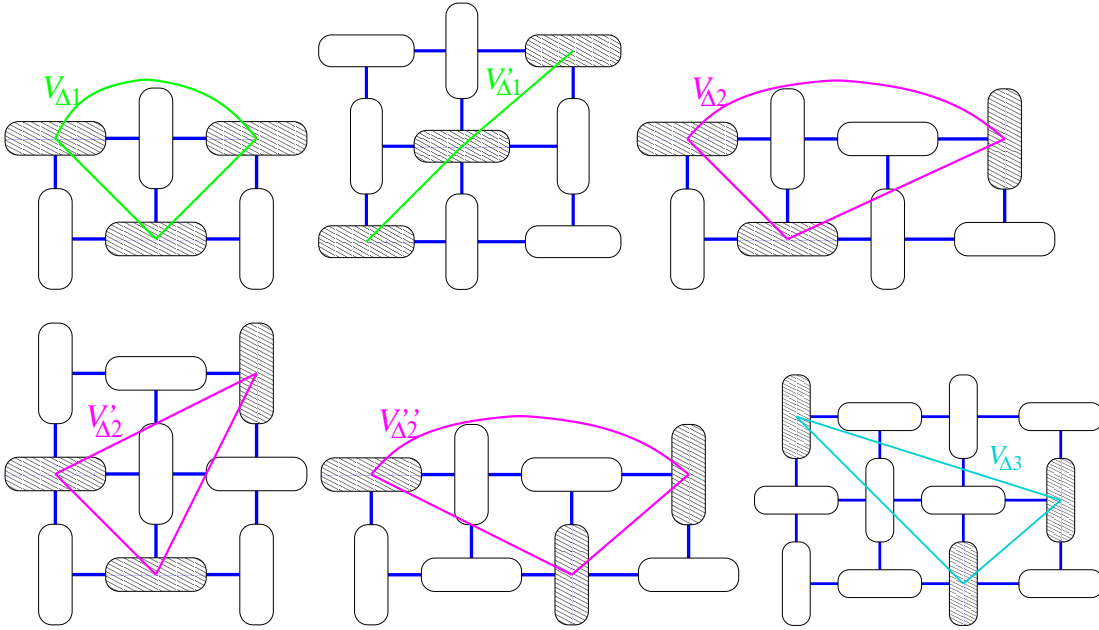


Figure 4: A schematic representation of effective three-particle interactions between triplons.

As a first step we have found the ground-state phase diagram of the spin-1/2 Heisenberg model on the Shastry-Sutherland lattice by ignoring the correlated hopping terms, which might seem to be irrelevant due to the strong repulsion between closely spaced triplons. The first fractional magnetization plateau, which appears while applying the magnetic field, is the 1/8-plateau. The relevant ground state corresponds to most dense packing of triplons, which avoids any repulsive pair and three-particle interactions between them as it is in the case of columnar or checkerboard orderings of triplons shown in Fig. 7 (a) and (b), respectively. It should be nevertheless mentioned that the 1/8-plateau phase corresponds to a highly degenerate ground-state manifold, because the translation of any row does not cost additional energy. Thus, the overall degeneracy of the 1/8-plateau phase is  $2^{N_x} + 2^{N_y}$ , where  $N_x$  and

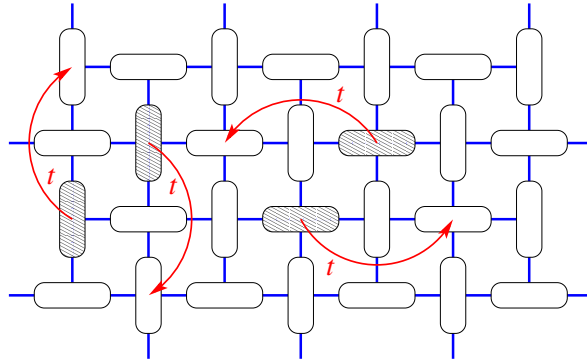


Figure 5: A schematic representation of the correlated hopping of two triplons, which are placed on two next-nearest-neighbor dimers.



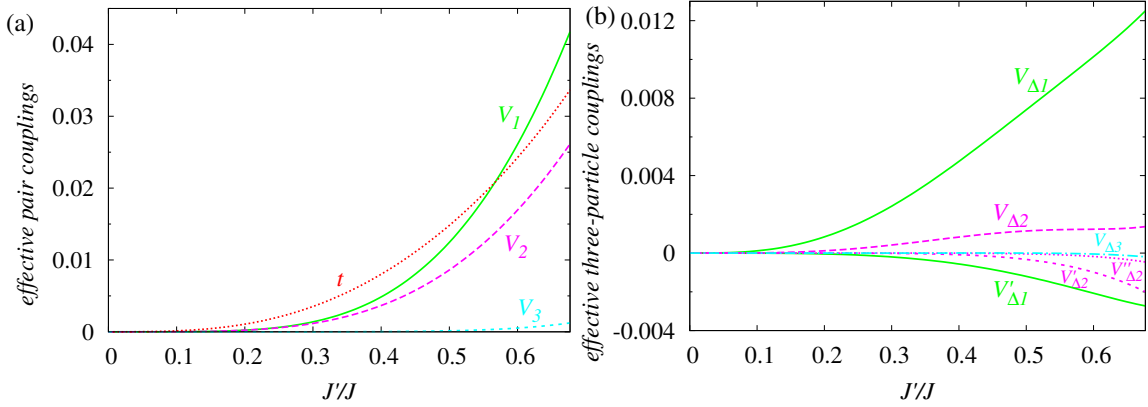


Figure 6: The effective pair (a) and three-particle (b) couplings (6) normalized with respect to the intradimer interaction  $J$  as a function of the relative size of the coupling constants  $J'/J$ . The correlated hopping term is shown in panel (a) as a dotted line together with the effective pair couplings.

$N_y$  determine the total number of dimers in  $x$  and  $y$  directions. Upon further increase of the magnetic field the  $1/6$ -plateau phase becomes favorable. The relevant ground state displays a striking columnar orderings of triplons developed either on the horizontal or vertical dimers, whereas the latter configuration is schematically shown in Fig. 7(c) for illustration. It is also worth mentioning that the  $2/15$ -plateau phase, which was identified in Refs. [6, 7], coexists together with the  $1/8$ - and  $1/6$ -plateau phases at their respective phase boundary. Hence, it is quite plausible to conjecture that the  $2/15$ -plateau phase may eventually emerge when the perturbation expansion would be developed to higher orders. The next consecutive ground state is the  $1/4$ -plateau phase, which exhibits a stripe-like arrangements of triplons either on vertical or horizontal dimers. Fig. 7(d) illustrates the particular case, where triplons have vertical disposition. Note that the stripe-like character of the  $1/4$ -plateau phase is ultimately connected to the effective three-particle interactions  $V_{\Delta 1}$  and  $V'_{\Delta 1}$ , because the zig-zag pattern of triplons has the same energy as the stripe one whenever the effective three-particle couplings  $V_{\Delta 1}$  and  $V'_{\Delta 1}$  are neglected. On the other hand, the effective three-particle interactions are much weaker than the pair ones and thus, the zig-zag configuration mentioned above may emerge even at comparably small temperatures. The last possible ground state within this picture is the  $1/3$ -plateau phase schematically illustrated in Fig. 2, which displays another stripe ordering of triplons being simultaneously the most dense packing of triplons satisfying the hard-core condition exemplified by red ovals in this figure. It could be thus concluded that the present consideration of the effective couplings between triplons leads to the emergence of three additional ground states emergent in between the singlet-dimer and stripe  $1/3$ -plateau phases (see Fig. 7).

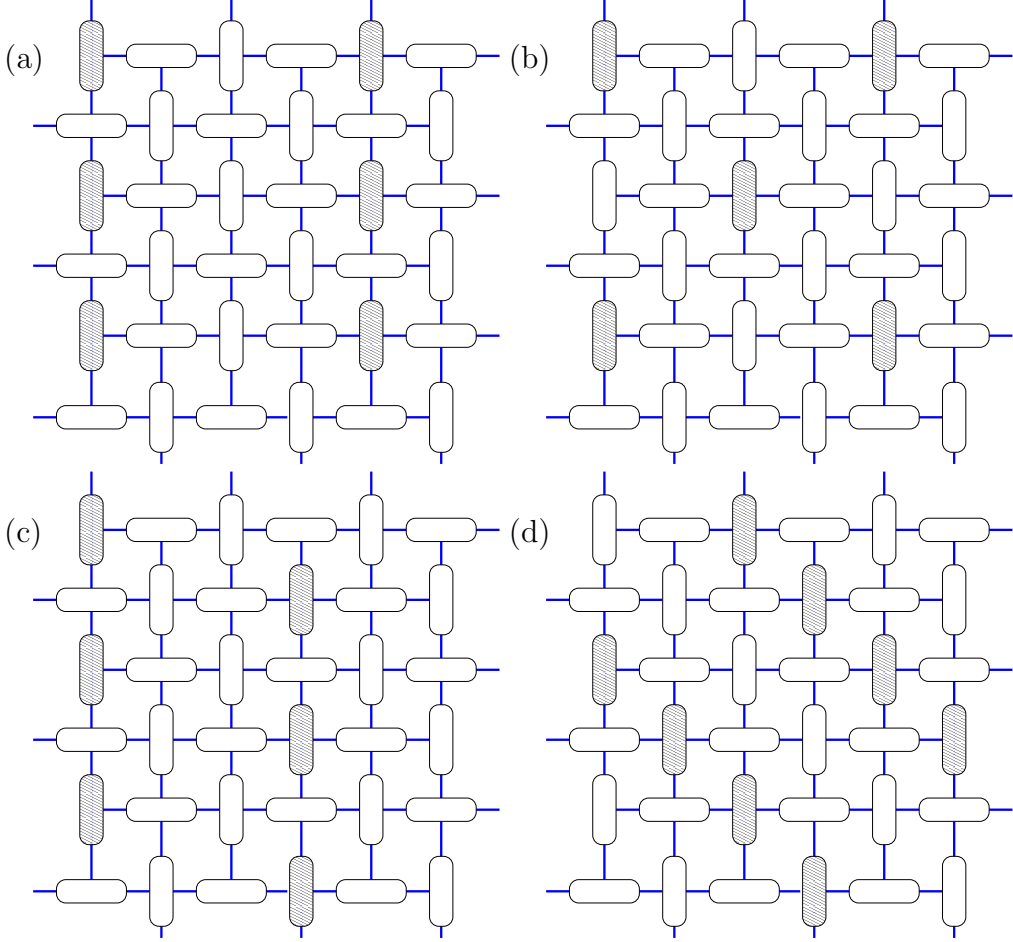


Figure 7: A schematic illustration of ground states of the spin-1/2 Heisenberg model on the Shastry-Sutherland lattice emergent in a low-field region as fractional magnetization plateaux: (a)-(b) 1/8-plateau [51]; (c) 1/6-plateau; (d) 1/4-plateau.

The ground-state energies of all aforementioned phases per one dimer read as follows:

$$\begin{aligned}
 E_{1/8} &= \frac{1}{8}(-h + h_{c1} + e_0), \\
 E_{1/6} &= \frac{1}{6}(-h + h_{c1} + e_0 + 2V_3), \\
 E_{1/4} &= \frac{1}{4}(-h + h_{c1} + e_0 + V_1 + V_3 + V'_{\Delta 1} + 2V_{\Delta 3}), \\
 E_{1/3} &= \frac{1}{3}(-h + h_{c1} + e_0 + V_1 + 2V_2 + V'_{\Delta 1} + 2(V_{\Delta 2} + V'_{\Delta 2} + V''_{\Delta 2})). \tag{7}
 \end{aligned}$$

It should be noted that all fractional-plateau phases are exact eigenstates of the effective Hamiltonian (6), whereas the 1/8- and 1/6-plateau phases contain the localized triplons only. On the other hand, the correlated hopping of triplons placed on next-nearest-neighbor dimers (see Fig. 5) is hypothetically possible in the 1/4- and 1/3-plateau phases although it is still suppressed due to a stripe arrangement of triplons satisfying the hard-core condition sketched

in Fig. 3. The critical fields delimiting phase boundaries between individual ground states can be readily found from a direct comparison of the respective eigenenergies given by Eqs. (7):

$$\begin{aligned}
h_{0-1/8} &= h_{c1} + e_0, \\
h_{1/8-1/6} &= h_{c1} + e_0 + 8V_3, \\
h_{1/6-1/4} &= h_{c1} + e_0 + 3V_1 - V_3 + 3V'_{\Delta 1} + 6V_{\Delta 3}, \\
h_{1/4-1/3} &= h_{c1} + e_0 + V_1 + 8V_2 - 3V_3 + V'_{\Delta 1} + 8(V_{\Delta 2} + V'_{\Delta 2} + V''_{\Delta 2}) - 6V_{\Delta 3}. \quad (8)
\end{aligned}$$

The critical fields (8) derived within the developed perturbation theory can be straightforwardly utilized for a construction of the overall ground-state phase diagram of the spin-1/2 Heisenberg model on the Shastry-Sutherland lattice, which is displayed in Fig. 8 in the  $J'/J - h/J$  plane together with available numerical data obtained previously using CORE [5] and iPEPS [10] methods. A direct comparison of the critical field  $h_{1/4-1/3}$  with the respective numerical data of CORE [5] and iPEPS [10] methods implies that the phase boundary between the 1/4- and 1/3-plateaux is reproduced by the newly developed perturbation scheme with an exceptional high accuracy up to the interaction ratio  $J'/J \approx 0.5$ . The phase boundary between 1/6- and 1/4-plateaux is also in a reasonable accordance with the result of the iPEPS method [10] even up to higher values of the interaction ratio  $J'/J \approx 0.6$ . The deviation of our results from the CORE method [5] for the phase boundary between the 1/6- and 1/8-plateaux might be explained by the finite-size limitations. The developed strong-coupling approach anticipates a relatively broad field range for the 1/6-plateau phase and a tiny field range for the 1/8-plateau phase, whereas the 2/15-plateau coexists at the phase boundary between the 1/8- and 1/6-plateaux. However, this finding seems to be in contradiction with the experimental observation for  $\text{SrCu}_2(\text{BO}_3)_2$  where a relatively broad 1/8-plateau was contrarily detected [26].

The obtained results open possibility to unambiguously determine the exchange couplings  $J$  and  $J'$  of  $\text{SrCu}_2(\text{BO}_3)_2$  according to the phase boundaries reported in Ref. [10]. It is clear from Fig. 8 that the phase boundaries of 1/4-plateau depend linearly on  $J'/J$  near plausible values of the interaction ratio  $J'/J \approx 0.6$ . Using the linear approximation for these phase boundaries and experimentally observed fields  $H_1^{exp} = 33$  T and  $H_2^{exp} = 39$  T, which determine lower bounds of the 1/4- and 1/3-plateaux of  $\text{SrCu}_2(\text{BO}_3)_2$ , one finds absolute values of the coupling constants  $J/k_B = 85.4$  K and  $J'/k_B = 54.1$  K. Note that these specific values of the coupling constants as well as a relative strength of the interaction ratio  $J'/J = 0.634$  are in a close coincidence with the previously reported fitting set of parameters gained from the temperature dependence of the magnetic susceptibility [52]. Next, the deduced coupling constants envisage for the phases with character of localized triplons the following critical field  $H_{1/6-1/4} = 33.03$  T between the 1/6- and 1/4-plateaux and  $H_{1/8-1/6} = 28.42$  T between the 1/8- and 1/6-plateaux, respectively. The energy of the localized triplon in zero field is found to be 43 K, which is slightly higher than the energy gap  $\Delta = 35$  K experimentally observed at zero magnetic field [51].

Last but not least, let us also briefly comment on the validity of our perturbation theory at small enough temperatures. The developed strong-coupling approach neglects possible excitations of dimers to the triplet states  $|2\rangle_1$ ,  $|3\rangle_1$  as well as the excitation of two triplons inside of the local cluster defined in Appendix A. The energy gap of the triplet excitation  $|1\rangle_1$  equals to  $J$ , while the creation of two triplons on the next-nearest-neighbor and further-neighbor dimers costs the energy  $(J' + \sqrt{J^2 + J'^2} - J)/2$  and  $(\sqrt{J^2 + J'^2} - J)$ , respectively. The last excitation is the smallest one for the inferred interaction ratio  $J'/J = 0.634$  and

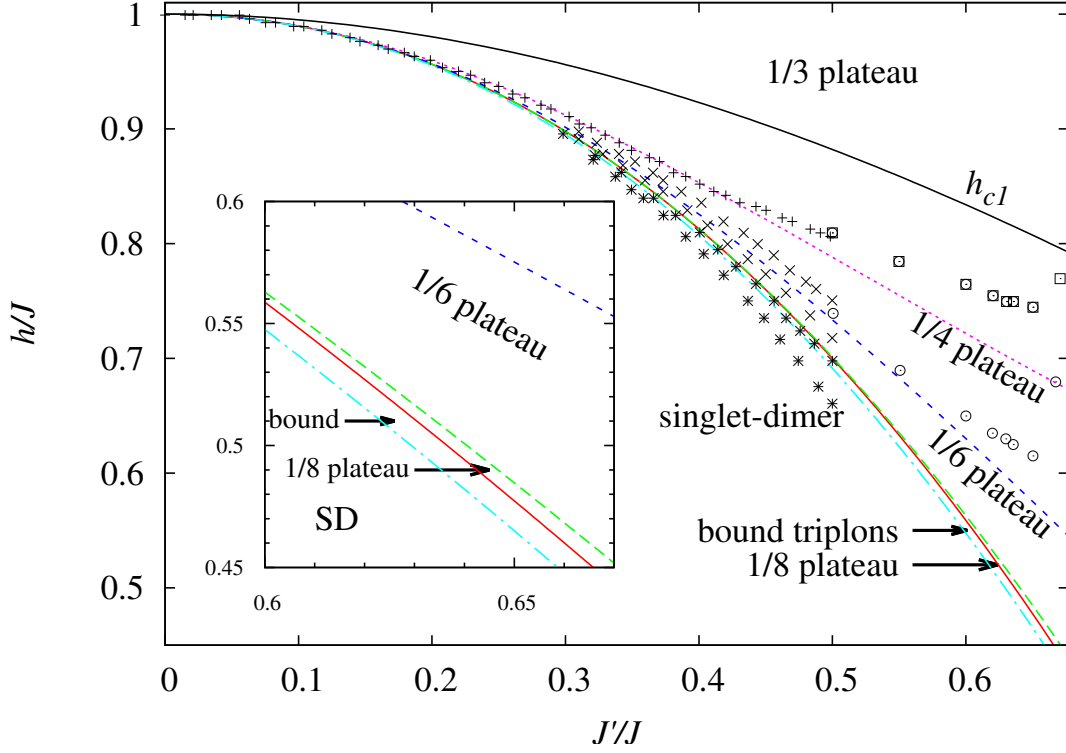


Figure 8: The ground-state phase diagram of the spin-1/2 Heisenberg model on the Shastry-Sutherland lattice in the  $J'/J - h/J$  plane. The critical fields (8) derived within the perturbation theory, which was developed from the exactly solved Ising-Heisenberg model up to the second order, are shown by lines of different styles. Symbols “+” display the phase boundary between the 1/4- and 1/3-plateaux, while the field range delimited by symbols “ $\times$ ” corresponds to the 1/6-plateau (for  $N = 36$  spins) and the field range delimited by symbols “ $*$ ” corresponds to the 1/8-plateau (for  $N = 32$  spins) obtained by the numerical CORE method [5]. Empty squares and circles show iPEPS results for lower critical fields of the 1/3- and 1/4-plateaux, respectively [10].

hence, one gets the energy gap of size  $\Delta = 0.18J/k_B$  (i.e.  $\Delta = 14.4$  K for  $J/k_B = 80$  K.) The values of the effective couplings are also useful to estimate the effect of temperature. It is apparent from Fig. 6 that some effective couplings are of order of a few Kelvins (e.g.  $V_1 \approx 0.04J/k_B \approx 3.2$  K,  $V_2 \approx 0.02*J/k_B \approx 1.5$  K), which means that the statistical weight of excited states might be high enough even at relatively low temperatures around 3 K in order to smooth the observed magnetization plateaux.

#### 4 Quantum correlated phase of bound triplons

The presence of the quantum hopping term and the extended hard-core repulsion make the solution of the full effective model (6) including the correlated hopping rather complicated. The mean-field approach is not capable of providing a proper description of the quantum motion of triplons with strong short-order bonding. In our case the correlated hopping could

be blocked by the strong repulsion between two triplons on next-nearest-neighbor dimers. On the other hand, a pair of bound triplons may gain even a lower energy due to the quantum correction terms. To analyze the possibility of an emergence of a two-triplon bound state, we consider a simplified model, where all states of localized triplons are excluded leaving only the possibility for the mobile pairs of triplons. For such a model one can devise the correspondence to the two-component hard-core Bose gas on the dual lattice (see Fig. 9) whose sites are defined at the center of pairs of dimers. Each site can be either empty or occupied by one of two kinds of hard-core bosons  $h$ -bosons (or  $v$ -bosons) representing a bound pair of triplons traveling along the horizontal (or vertical) direction. These bosons obey the following hard-core conditions: first, no more than one boson is allowed on a site, second, each boson on site  $(i, j)$  forbids the occupation of neighboring sites according to the hard-core condition of separate triplons (see also red circles in Fig. 9). These conditions can be fulfilled by the following projection operators:

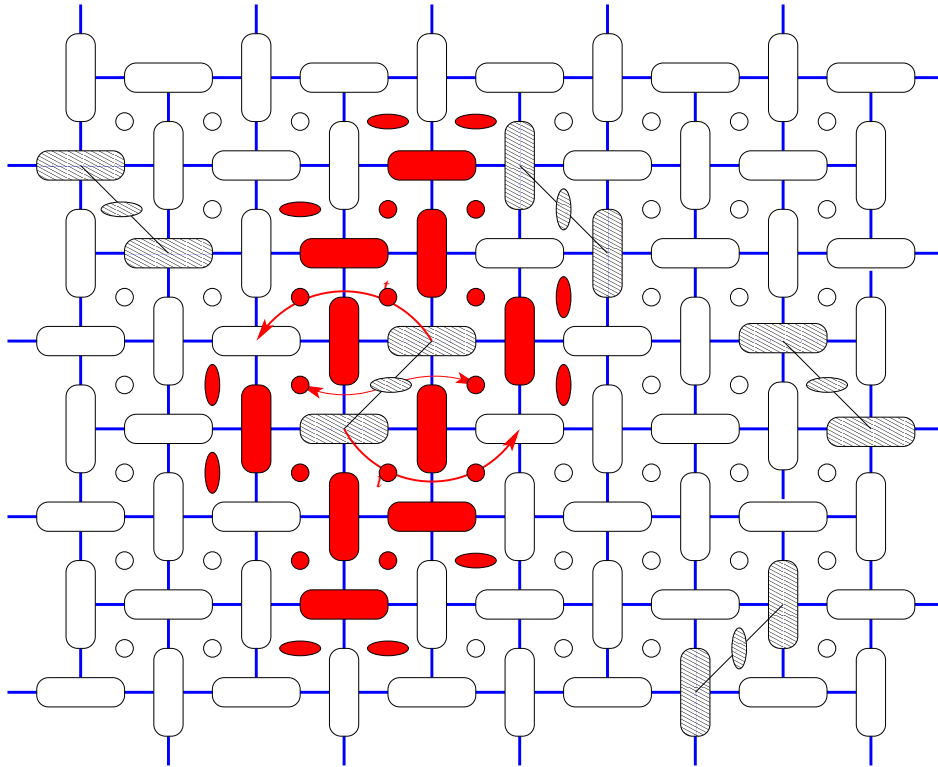


Figure 9: The effective model for bound triplons. Small circles and ellipses denote sites of the dual lattice. The empty circle corresponds to the empty site, horizontally (vertically) oriented ellipses mark the bound state of two triplons in the horizontal (vertical) direction. The hard-core condition for a given two-triplon state is outlined by red circles (sites are forbidden for any boson) and red horizontal or vertical ellipse (site is forbidden for the horizontal or vertical boson).

$$\begin{aligned}
\mathcal{P}_{i,j,h} &= (1 - n_{i,j,h}n_{i,j,v})\bar{n}_{i-1,j-1}\bar{n}_{i,j-1}\bar{n}_{i+1,j-1}\bar{n}_{i+1,j}\bar{n}_{i+1,j+1}\bar{n}_{i,j+1}\bar{n}_{i-1,j+1}\bar{n}_{i-1,j} \\
&\quad \times \bar{n}_{i-1,j-2}\bar{n}_{i,j-2}\bar{n}_{i+1,j+2}\bar{n}_{i-1,j-3,h}\bar{n}_{i,j-3,h}\bar{n}_{i+1,j-2,h} \\
&\quad \times \bar{n}_{i-1,j+2,h}\bar{n}_{i,j+3,h}\bar{n}_{i+1,j+3,h}\bar{n}_{i-2,j-1,v}\bar{n}_{i-2,j,v}\bar{n}_{i+2,j,v}\bar{n}_{i+2,j+1,v}, \text{ if } i+j = \text{odd}, \\
\mathcal{P}_{i,j,h} &= (1 - n_{i,j,h}n_{i,j,v})\bar{n}_{i-1,j-1}\bar{n}_{i,j-1}\bar{n}_{i+1,j-1}\bar{n}_{i+1,j}\bar{n}_{i+1,j+1}\bar{n}_{i,j+1}\bar{n}_{i-1,j+1}\bar{n}_{i-1,j} \\
&\quad \times \bar{n}_{i,j-2}\bar{n}_{i+1,j-2}\bar{n}_{i-1,j+2}\bar{n}_{i,j+2}\bar{n}_{i-1,j-2,h}\bar{n}_{i,j-3,h}\bar{n}_{i+1,j-3,h} \\
&\quad \times \bar{n}_{i-1,j+3,h}\bar{n}_{i,j+3,h}\bar{n}_{i+1,j+2,h}\bar{n}_{i-2,j,v}\bar{n}_{i-2,j+1,v}\bar{n}_{i+2,j-1,v}\bar{n}_{i+2,j,v}, \text{ if } i+j = \text{even}, \\
\bar{n}_{i,j,v} &= 1 - n_{i,j,v}, \quad \bar{n}_{i,j} = \bar{n}_{i,j,h} + \bar{n}_{i,j,v}. \tag{9}
\end{aligned}$$

$\mathcal{P}_{i,j,v}$  can be deduced from Eq. (9) by interchanging indices  $i$  and  $j$ . Since triplons in a pair can move along its orientation only, the corresponding quasiparticle is able to travel in the same direction. Now one can see that the hopping of a triplon between sites can be presented as a jump of a quasiparticle identified on the dual lattice. Finally, one arrives at the following Hamiltonian:

$$\begin{aligned}
H_{\text{bound}} &= P \sum_{i,j} \{t(b_{i,j,h}^+ b_{i+1,j,h} + b_{i+1,j,h}^+ b_{i,j,h} + b_{i,j,v}^+ b_{i,j+1,v} + b_{i,j+1,v}^+ b_{i,j,v}) \\
&\quad + (2(e_0 + h_1 - h) + V_1) \sum_{\alpha=h,v} n_{i,j,\alpha} + (V_1 + 2V_{\Delta 1})(n_{i,j,h}n_{i+2,j,h} + n_{i,j,v}n_{i,j+2,v}) \\
&\quad + (V_1 + V_{\Delta 1} + V'_{\Delta 1})(n_{i,j,h}n_{i+2,j+1,h} + n_{i,j,h}n_{i+2,j-1,h} + n_{i,j,v}n_{i+1,j+2,v} \\
&\quad + n_{i,j,v}n_{i-1,j+2,v})\}P, \tag{10}
\end{aligned}$$

where  $b_{i,j,\alpha}^+$  ( $b_{i,j,\alpha}$ ) creates (annihilates) a pair of triplons in  $\alpha = h, v$  direction.

Next, it is useful to estimate the critical field required for the emergence of the quantum state of bound triplons. In the particular case of one boson, the spectrum of the quasi-particle excitations can be found as follows:

$$\epsilon(\kappa) = 2t \cos(\kappa) + 2(e_0 + h_{c1} - h) + V_1. \tag{11}$$

where  $\kappa = 2\pi l/N_x$  ( $\kappa = 2\pi l/N_y$ ) for  $h$ -bosons ( $v$ -bosons) and  $l = 0, 1, \dots, N_x(N_y)$ . Hence, it might be useful to compare the minimal energy of the wave of the bound triplons  $\epsilon(\pi) = -2t + 2(e_0 + h_{c1} - h) + V_1$  with the energy of two separate triplons  $2E_{\text{triplon}} = 2(e_0 + h_{c1} - h)$ . The difference of two energies is displayed in Fig. 10, which shows that the wave of the bound triplons always have lower energy than the localized triplons. Owing to this fact, the quantum phase of bound triplons should appear at low enough magnetic fields prior to the crystal of localized triplon phases. The critical field for the emergence of the quantum bound-triplon phase at sufficiently low magnetic fields is given by  $h_{\text{quant}} = e_0 + h_{c1} - t + V_1/2$ . At this critical field the stripe-like phases of delocalized bound-triplons should evolve. Moreover, the wave of bound triplons should be separated due to the special hard-core repulsion (see Fig. 2 and its description in the text) by three consecutive rows of singlet-like dimers. Such a picture is reminiscent of the 1/8-plateau phase revealed in the Shastry-Sutherland model on a tube geometry with the four dimers in the transverse direction [8]. In the latter case it is implemented as a wheel state of bound triplons. It is natural to suppose that by extending the width of the tube to infinity this state become identical to the stripe-phase of delocalized bound-triplons suggested above. It should be also mentioned that the emergence of bound triplet states in the Shastry-Sutherland model was initially discussed in Refs. [13–16]. Recently, the possibility of the stripe magnetic ordering of bound triplons has

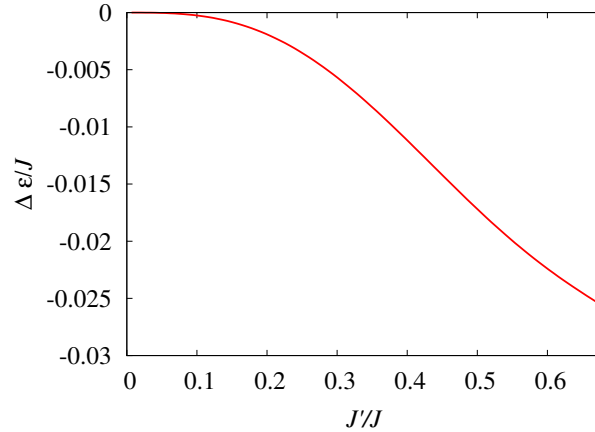


Figure 10: The energy difference between the bound triplons and two localized triplons.

been devised in Ref. [20]. The relevant phase boundary of the quantum bound-triplon phase is plotted in the ground-state phase diagram together with all other phase boundaries (see also inset in Fig. 8). It is quite evident that a stability region of the quantum bound-triplon phase is limited to a very narrow range of the magnetic fields and moreover, the behavior of this quantum phase at larger magnetic fields is highly uncertain and would require a more comprehensive study.

## 5 Conclusions

In the present paper we have elaborated an approximate method for the spin-1/2 Heisenberg model on the Shastry-Sutherland lattice, which relies on the perturbative treatment of  $XY$  part of the interdimer coupling. The spin-1/2 Ising-Heisenberg model on the Shastry-Sutherland lattice has been used as a useful starting ground (unperturbed reference system), for which the ground state is known exactly [47]. Our particular attention has been focused on a range of sufficiently low magnetic fields, which magnetize the system up to the intermediate 1/3-plateau when the magnetization is scaled with respect to the saturation value. Within the second order of the many-body perturbation theory, we have obtained an effective lattice-gas model for the triplon excitations with the special hard-core repulsion, which recovers presence of the fractional 1/8-, 1/6- and 1/4-plateaux. The nature of ground states pertinent to these fractional magnetization plateaux was clarified in detail and it either corresponds to columnar or stripe orderings of localized triplons. Moreover, the stripe ordering of triplons in the 1/4-plateau phase is stabilized by a small three-particle interaction. Therefore, the zig-zag ordering of triplons may also eventually emerge within the 1/4-plateau at relatively low temperatures due to the thermal activation of this low-lying excited state. In addition, it has been found that the 2/15-plateau phase coexists at the phase boundary between the 1/8- and 1/6-plateaux and it may therefore gain a finite width in higher orders of the perturbation theory.

It is noteworthy that the derived critical fields for the fractional magnetization plateaux are in a good agreement with the available numerical data when the respective deviation is less

than 5%. The linear dependence of the critical field near the presumed ratio of the coupling constants  $J'/J \sim 0.6$  has allowed us to refine the coupling constants from the phase boundary of the 1/4-plateau observed experimentally in Refs. [10, 27]. A reliable agreement with the experimental data were also found when comparing the critical fields for other fractional magnetization plateaux with the ones detected in  $\text{SrCu}_2(\text{BO}_3)_2$  [10, 26, 27]. In addition, it turns out that the calculated energy of the localized triplon excitations only slightly overestimates the energy gap of  $\text{SrCu}_2(\text{BO}_3)_2$  experimentally observed in zero magnetic field. Finally, the importance of quantum terms in the form of the correlated hopping process has been analyzed. It has been demonstrated that the correlated hopping may give rise to the creation of the bound pair of triplons with much lower energy in comparison with two localized triplons. Thus, a stripe-like order of the delocalized bound triplons is presumed to evolve at sufficiently low magnetic fields. This conjecture might be of considerable interest for future experimental testing.

## Acknowledgements

The authors are grateful to F. Mila and K.P. Schmidt for useful discussions.

**Funding information** T.V. acknowledges the financial support provided by the National Scholarship Programme of the Slovak Republic for the Support of Mobility of Students, PhD Students, University Teachers, Researchers and Artists. J.S. acknowledges financial support provided by the grant The Ministry of Education, Science, Research and Sport of the Slovak Republic under the contract No. VEGA 1/0105/20 and by the grant of the Slovak Research and Development Agency under the contract No. APVV-16-0186.

## A Diagonalization of the Ising-Heisenberg model

In this part, we will derive the exact ground state of the spin-1/2 Ising-Heisenberg model on the Shastry-Sutherland lattice using the formalism of the projection operators [53, 54]  $A_{i,j}^{ab} = |a\rangle_{i,j}\langle b|_{i,j}$ , where  $|a\rangle_{i,j}$  and  $\langle b|_{i,j}$  are the dimer states defined by Eq. (3). For the sake of clarity, it is better to consider the relevant Hamiltonian (2) in the notation of full indices [47]:

$$\begin{aligned}
 H_{IH} &= \sum'_{i,j=1}^N H_{i,[j-1:j+1]} + \sum''_{i,j=1}^N H_{[i-1:i+1],j}, \\
 H_{[i-1:i+1],j} &= J(\mathbf{s}_{1,i,j} \cdot \mathbf{s}_{2,i,j}) + J'(S_{i-1,j}^z s_{1,i,j}^z + s_{2,i,j}^z S_{i+1,j}^z) - hS_{i,j}^z, \\
 H_{i,[j-1:j+1]} &= J(\mathbf{s}_{1,i,j} \cdot \mathbf{s}_{2,i,j}) + J'(S_{i,j-1}^z s_{1,i,j}^z + s_{2,i,j}^z S_{i,j+1}^z) - hS_{i,j}^z,
 \end{aligned} \tag{12}$$

where  $\sum'$  ( $\sum''$ ) is restricted by the constraint  $i + j = \text{odd}$  ( $i + j = \text{even}$ ). The cluster Hamiltonians (12) can be rewritten in terms of the introduced projection operators into the following form (see Ref. [55] for the similar representation of the spin-1/2 Ising-Heisenberg



orthogonal-dimer chain):

$$\begin{aligned}
H_{[i-1:i+1],j} &= J \left( \frac{1}{4} - A_{ij}^{00} \right) - h S_{ij}^z + \frac{J'}{2} \left[ (S_{i-1,j}^z + S_{i+1,j}^z) S_{ij}^z + (S_{i-1,j}^z - S_{i+1,j}^z) (A_{ij}^{20} + A_{ij}^{02}) \right], \\
H_{i,[j-1:j+1]} &= J \left( \frac{1}{4} - A_{ij}^{00} \right) - h S_{ij}^z + \frac{J'}{2} \left[ (S_{i,j-1}^z + S_{i,j+1}^z) S_{ij}^z + (S_{i,j-1}^z - S_{i,j+1}^z) (A_{ij}^{20} + A_{ij}^{02}) \right]. \quad (13)
\end{aligned}$$

For compactness, we have preserved the spin operator  $S_{i,j}^z = A_{i,j}^{11} - A_{i,j}^{33}$  in the cluster Hamiltonians (13). It can be readily proved that all local Hamiltonians (13) commute with each other and, therefore, they can be diagonalized independently. Following Refs. [47, 55] it is advisable to define the unitary transformation  $U_{i,j}^\nu$  ( $\nu = h, v$  denote either horizontal or vertical orientation of the central dimer in a cluster):

$$\begin{aligned}
U_{i,j}^\nu &= (A_{i,j}^{11} + A_{i,j}^{33}) + \cos \frac{\alpha_{i,j}^\nu}{2} (A_{i,j}^{00} + A_{i,j}^{22}) + \sin \frac{\alpha_{i,j}^\nu}{2} (A_{i,j}^{20} - A_{i,j}^{02}), \\
\cos \alpha_{i,j}^h &= \frac{J}{\sqrt{J^2 + J'^2 (S_{i-1,j}^z - S_{i+1,j}^z)^2}}, \quad \sin \alpha_{i,j}^h = \frac{J' (S_{i-1,j}^z - S_{i+1,j}^z)}{\sqrt{J^2 + J'^2 (S_{i-1,j}^z - S_{i+1,j}^z)^2}}, \quad \text{if } i+j = \text{even}, \\
\cos \alpha_{i,j}^v &= \frac{J}{\sqrt{J^2 + J'^2 (S_{i,j-1}^z - S_{i,j+1}^z)^2}}, \quad \sin \alpha_{i,j}^v = \frac{J' (S_{i,j-1}^z - S_{i,j+1}^z)}{\sqrt{J^2 + J'^2 (S_{i,j-1}^z - S_{i,j+1}^z)^2}}, \quad \text{if } i+j = \text{odd}, \\
\cos \frac{\alpha_{i,j}^h}{2} &= \sqrt{\frac{1 + \cos \alpha_{i,j}^h}{2}} = 1 + (c_1^+ - 1) P_{|1|} (S_{i-1,j}^z - S_{i+1,j}^z) + (c_2^+ - 1) P_{|2|} (S_{i-1,j}^z - S_{i+1,j}^z), \\
\sin \frac{\alpha_{i,j}^h}{2} &= \text{sgn}(\sin \alpha_{i,j}^h) \sqrt{\frac{1 - \cos \alpha_{i,j}^h}{2}} = c_1^- P_{\pm 1} (S_{i-1,j}^z - S_{i+1,j}^z) + c_2^- P_{\pm 2} (S_{i-1,j}^z - S_{i+1,j}^z), \\
\cos \frac{\alpha_{i,j}^v}{2} &= 1 + (c_1^+ - 1) P_{|1|} (S_{i,j-1}^z - S_{i,j+1}^z) + (c_2^+ - 1) P_{|2|} (S_{i,j-1}^z - S_{i,j+1}^z), \\
\sin \frac{\alpha_{i,j}^v}{2} &= c_1^- P_{\pm 1} (S_{i,j-1}^z - S_{i,j+1}^z) + c_2^- P_{\pm 2} (S_{i,j-1}^z - S_{i,j+1}^z), \\
c_1^\pm &= \frac{1}{\sqrt{2}} \sqrt{1 \pm \frac{J}{\sqrt{J^2 + J'^2}}}, \quad c_2^\pm = \frac{1}{\sqrt{2}} \sqrt{1 \pm \frac{J}{\sqrt{J^2 + 4J'^2}}}, \\
P_{|1|} (S_{i,j}^z - S_{i',j'}^z) &= \delta(|S_{i,j}^z - S_{i',j'}^z| - 1) = (A_{i,j}^{11} + A_{i,j}^{33})(A_{i',j'}^{00} + A_{i',j'}^{22}) + (A_{i,j}^{00} + A_{i,j}^{22})(A_{i',j'}^{11} + A_{i',j'}^{33}), \\
P_{|2|} (S_{i,j}^z - S_{i',j'}^z) &= \delta(|S_{i,j}^z - S_{i',j'}^z| - 2) = A_{i,j}^{11} A_{i',j'}^{33} + A_{i,j}^{33} A_{i',j'}^{11}, \\
P_{\pm 1} (S_{i,j}^z - S_{i',j'}^z) &= (S_{i,j}^z - S_{i',j'}^z) \delta(|S_{i,j}^z - S_{i',j'}^z| - 1) \\
&= (A_{i,j}^{11} - A_{i,j}^{33})(A_{i',j'}^{00} + A_{i',j'}^{22}) - (A_{i,j}^{00} + A_{i,j}^{22})(A_{i',j'}^{11} - A_{i',j'}^{33}), \\
P_{\pm 2} (S_{i,j}^z - S_{i',j'}^z) &= \frac{1}{2} (S_{i,j}^z - S_{i',j'}^z) \delta(|S_{i,j}^z - S_{i',j'}^z| - 2) = A_{i,j}^{11} A_{i',j'}^{33} - A_{i,j}^{33} A_{i',j'}^{11}, \quad (14)
\end{aligned}$$

where  $\delta(\dots)$  denotes the Kronecker symbol. One can check that the unitary transformation  $U_{i,j}^\nu$  removes all non-diagonal operators from the cluster Hamiltonians (13) what results in a "classical" (fully diagonal) representation of the Hamiltonian of the spin-1/2 Ising-Heisenberg

model on the Shastry-Sutherland lattice [47]:

$$\begin{aligned}
\tilde{H}_{[i-1:i+1],j} &= U_{i,j} H_{[i-1:i+1],j} U_{i,j}^+ = \left( \frac{J'}{2} (S_{i-1,j}^z + S_{i+1,j}^z) - h \right) S_{ij}^z + J \left( \frac{1}{4} - A_{ij}^{00} \right) \\
&\quad + \frac{1}{2} I (|S_{i-1,j}^z - S_{i+1,j}^z|) (A_{ij}^{22} - A_{ij}^{00}), \\
\tilde{H}_{i,[j-1:j+1]} &= U_{i,j} H_{i,[j-1:j+1]} U_{i,j}^+ = \left( \frac{J'}{2} (S_{i,j-1}^z + S_{i,j+1}^z) - h \right) S_{ij}^z + J \left( \frac{1}{4} - A_{ij}^{00} \right) \\
&\quad + \frac{1}{2} I (|S_{i,j-1}^z - S_{i,j+1}^z|) (A_{ij}^{22} - A_{ij}^{00}), \\
I(|S_{i+1,j}^z - S_{i-1,j}^z|) &= \sqrt{J^2 + J'^2 (S_{i+1,j}^z - S_{i-1,j}^z)^2} - J.
\end{aligned} \tag{15}$$

All ground states of the Hamiltonian (15) were found in Ref. [47], to which readers interested in further details are referred to.

## B Technical details of the perturbation theory

Let us start with the brief reference of the many-body perturbation theory adapted according to Ref. [49]. Within this scheme, it is convenient to decompose the total Hamiltonian into the unperturbed part  $H_0$  and the perturbed part  $H'$ :

$$H = H_0 + \lambda H', \tag{16}$$

whereas the eigenvalue problem for the unperturbed part of the Hamiltonian  $H_0 |\Phi_i\rangle = E_i^{(0)} |\Phi_i\rangle$  should be rigorously tractable. If  $\mathcal{P}_i$  is the projection into the unperturbed model space  $H_0$  and  $\mathcal{Q}_i = 1 - \mathcal{P}_i$ , then, one gets within the perturbation theory:

$$\begin{aligned}
H_{eff} &= \mathcal{P}_i H \mathcal{P}_i + \lambda^2 \mathcal{P}_i H' R_s \sum_{n=0}^{\infty} [(H' - \delta E_i) R_s]^n \mathcal{Q}_i H' \mathcal{P}_i, \\
R_s &= \mathcal{Q}_i \frac{1}{E_i - H_0} = \sum_{m \neq i} \frac{|\Phi_m\rangle \langle \Phi_m|}{E_i - E_m^{(0)}} = \sum_{m \neq i} \frac{\mathcal{P}_m}{E_i - E_m^{(0)}},
\end{aligned} \tag{17}$$

where  $\delta E_i = E_i - E_i^{(0)}$  and  $E_i$  is the energy eigenvalue corresponding the state  $|\Phi_i\rangle$ . Thus, one obtains from the perturbation expansion (17) the following effective Hamiltonians  $H_{eff}^{(0)} = \mathcal{P}_0 H_0 \mathcal{P}_0$ ,  $H_{eff}^{(1)} = \lambda \mathcal{P}_0 H' \mathcal{P}_0$ ,  $H_{eff}^{(2)} = \lambda^2 \mathcal{P}_0 H' R_s H' \mathcal{P}_0$ , whereas the effective Hamiltonian  $H_{eff}^{(n)}$  denotes the  $n$ -th order of the perturbation expansion (17).

In particular, we will consider here the perturbation about the phase boundary between the singlet-dimer and stripe 1/3-plateau phase of the spin-1/2 Ising-Heisenberg model on the Shastry-Sutherland lattice emergent at the critical field  $h_{c1} = -\sqrt{J^2 + J'^2} + 2J$  [47]. The ideal part  $H^{(0)}$  of the Hamiltonian was chosen as the Ising-Heisenberg model (12) at the critical field  $h_{c1}$ , whereas the deviation from the critical field and the  $XY$  part of the interdimer

coupling goes into the perturbed part  $H'$ :

$$\begin{aligned}
H' &= \sum'_{i,j=1}^N H'_{i,j} + \sum''_{i,j=1}^N H''_{i,j}, \\
H'_{i,j} &= \frac{J'_{xy}}{2} \left[ S_{i,j}^+ (s_{1,i,j-1}^- + s_{2,i,j-1}^-) + S_{i,j}^- (s_{1,i,j-1}^+ + s_{2,i,j-1}^+) \right] - (h - h_{c1}) S_{i,j}^z, \\
H''_{i,j} &= \frac{J'_{xy}}{2} \left[ S_{i,j}^+ (s_{1,i+1,j}^- + s_{2,i-1,j}^-) + S_{i,j}^- (s_{1,i+1,j}^+ + s_{2,i-1,j}^+) \right] - (h - h_{c1}) S_{i,j}^z, \quad (18)
\end{aligned}$$

where we have introduced the spin raising and lowering operators  $s_{l,i,j}^\pm = s_{l,i,j}^x \pm i s_{l,i,j}^y$ ,  $H'_{i,j}$  and  $H''_{i,j}$  correspond to the condition  $i + j = \text{odd}$  and  $i + j = \text{even}$ , respectively. As it was proved in Ref. [47], the ground state is the lattice gas of triplons with the hard-core repulsion given in Fig. 2. Henceforth, we will exploit the projection operators defined in Appendix A instead of the spin operators. The hard-core condition can be implemented by the following projection operator:

$$\begin{aligned}
\mathcal{P}_0 &= \prod'_{i,j=1}^N (A_{i,j}^{00} + A_{i,j}^{11} P_{ij}^h) \prod''_{i,j=1}^N (A_{i,j}^{00} + A_{i,j}^{11} P_{ij}^v), \\
P_{ij}^h &= A_{i,j-1}^{00} A_{i,j+1}^{00} A_{i-2,j}^{00} A_{i-1,j}^{00} A_{i+1,j}^{00} A_{i+2,j}^{00}, \\
P_{ij}^v &= A_{i-1,j}^{00} A_{i+1,j}^{00} A_{i,j-2}^{00} A_{i,j-1}^{00} A_{i,j+1}^{00} A_{i,j+2}^{00}. \quad (19)
\end{aligned}$$

It should be noted that the perturbation expansion needs to be performed for the unitary transformed operators  $\tilde{O} = U O U^+$ , where  $U = \left( \prod' U_{i,j} \right) \left( \prod'' U_{i,j} \right)$ . In this case, the Hamiltonian of the Ising-Heisenberg model gains a fully diagonal form as given by Eq. (15). The perturbation approach is valid for  $J' < 0.678J$ , where the zero-field ground state consists of a product of singlet dimers [3].

The first-order term is the perturbation operator projected on the subspace (19)  $H^{(1)} = P U H' U^+ P$ . The field term gives the only contribution here:

$$H_{eff}^{(1)} = (h_{c1} - h) \sum_{i,j} A_{i,j}^{11} \mathcal{P}_0. \quad (20)$$

The second-order term follows directly from Eq. (17):

$$H^{(2)} = \sum_{m \neq 0} \frac{\mathcal{P}_0 U H' U^+ \mathcal{P}_m U H' U^+ \mathcal{P}_0}{E_0^{(0)} - E_m^{(0)}} \quad (21)$$

It is useful to be decompose the tedious calculation into more elemental parts. We start with

the calculations of the following expressions explicitly ( $(i+j) = \text{even}$ ):

$$\begin{aligned}
Us_{1,i,j+1}^+ S_{i,j}^- U^+ \mathcal{P}_0 &= -(c_1^+ + c_1^-) A_{i,j}^{21} (c_1^+ A_{i,j-1}^{00} + c_1^- A_{i,j-1}^{20}) \tilde{A}_{i,j+1}^{10} \mathcal{P}_0 \\
&\quad + c_1^- (A_{i-1,j}^{11} - A_{i+1,j}^{11}) \tilde{A}_{i,j}^{30} \tilde{A}_{i,j+1}^{10} (A_{i,j+2}^{00} + (c_1^+ - c_1^-) A_{i,j+2}^{11}) \mathcal{P}_0, \\
Us_{2,i,j-1}^+ S_{i,j}^- U^+ \mathcal{P}_0 &= (c_1^+ + c_1^-) A_{i,j}^{21} (c_1^+ A_{i,j+1}^{00} + c_1^- A_{i,j+1}^{20}) \tilde{A}_{i,j-1}^{10} \mathcal{P}_0 \\
&\quad - c_1^- (A_{i-1,j}^{11} - A_{i+1,j}^{11}) \tilde{A}_{i,j}^{30} \tilde{A}_{i,j-1}^{10} (A_{i,j-2}^{00} + (c_1^+ - c_1^-) A_{i,j-2}^{11}) \mathcal{P}_0, \\
\tilde{A}_{i,j}^{30} &= A_{i,j}^{30} [A_{i,j-2}^{00} (A_{i,j-1}^{11} + c_1^+ A_{i,j-1}^{00} + c_1^- A_{i,j-1}^{20}) \\
&\quad + A_{i,j-2}^{11} \{(c_1^+ c_2^+ + c_1^- c_2^-) A_{i,j-1}^{00} + (c_1^+ c_2^- - c_1^- c_2^+) A_{i,j-1}^{20}\}], \\
\tilde{\tilde{A}}_{i,j}^{30} &= A_{i,j}^{30} [A_{i,j+1}^{11} + A_{i,j+2}^{00} (c_1^+ A_{i,j+1}^{00} + c_1^- A_{i,j+1}^{20}) \\
&\quad + A_{i,j+2}^{11} \{(c_1^+ c_2^+ + c_1^- c_2^-) A_{i,j+1}^{00} - (c_1^+ c_2^- - c_1^- c_2^+) A_{i,j+1}^{20}\}], \\
\tilde{A}_{i,j\pm 1}^{10} &= A_{i,j\pm 1}^{10} (A_{i-1,j\pm 1}^{11} + c_1^+ A_{i-1,j\pm 1}^{00} - c_1^- A_{i-1,j\pm 1}^{20}) (A_{i+1,j\pm 1}^{11} + c_1^+ A_{i+1,j\pm 1}^{00} - c_1^- A_{i+1,j\pm 1}^{20}), \quad (22)
\end{aligned}$$

$$\begin{aligned}
Us_{1,i,j+1}^- S_{i,j}^+ U^+ \mathcal{P}_0 &= -c_1^- A_{i,j}^{10} (A_{i-1,j}^{11} - A_{i+1,j}^{11}) (A_{i,j-1}^{11} + c_1^+ A_{i,j-1}^{00} - c_1^- A_{i,j-1}^{20}) \\
&\quad \times \{(A_{i,j+2}^{00} + (c_1^+ + c_1^-) A_{i,j+2}^{11}) \tilde{A}_{i,j+1}^{30} + [-(c_1^+ + c_1^-) A_{i,j+1}^{01} + (c_1^+ - c_1^-) A_{i,j+1}^{21}] \\
&\quad \times (c_1^+ A_{i-1,j+1}^{00} + c_1^- A_{i-1,j+1}^{20}) (c_1^+ A_{i+1,j+1}^{00} - c_1^- A_{i+1,j+1}^{20})\} \mathcal{P}_0 \\
Us_{2,i,j-1}^- S_{i,j}^+ U^+ \mathcal{P}_0 &= -c_1^- A_{i,j}^{10} (A_{i-1,j}^{11} - A_{i+1,j}^{11}) (A_{i,j+1}^{11} + c_1^+ A_{i,j+1}^{00} + c_1^- A_{i,j+1}^{20}) \\
&\quad \times \{-(A_{i,j-2}^{00} + (c_1^+ + c_1^-) A_{i,j-2}^{11}) \tilde{A}_{i,j-1}^{30} + [(c_1^+ + c_1^-) A_{i,j-1}^{01} + (c_1^+ - c_1^-) A_{i,j-1}^{21}] \\
&\quad \times (c_1^+ A_{i-1,j-1}^{00} + c_1^- A_{i-1,j-1}^{20}) (c_1^+ A_{i+1,j-1}^{00} - c_1^- A_{i+1,j-1}^{20})\} \mathcal{P}_0 \\
\tilde{\tilde{A}}_{i,j\pm 1}^{30} &= A_{i,j\pm 1}^{30} [A_{i+1,j\pm 1}^{11} + A_{i+2,j\pm 1}^{00} (c_1^+ A_{i+1,j\pm 1}^{00} - c_1^- A_{i+1,j\pm 1}^{20}) \\
&\quad + A_{i+2,j\pm 1}^{11} \{(c_1^+ c_2^+ + c_1^- c_2^-) A_{i+1,j\pm 1}^{00} - (c_1^+ c_2^- - c_1^- c_2^+) A_{i+1,j\pm 1}^{20}\}] \\
&\quad \times [A_{i-1,j\pm 1}^{11} + A_{i-2,j\pm 1}^{00} (c_1^+ A_{i-1,j\pm 1}^{00} + c_1^- A_{i-1,j\pm 1}^{20}) \\
&\quad + A_{i-2,j\pm 1}^{11} \{(c_1^+ c_2^+ + c_1^- c_2^-) A_{i-1,j\pm 1}^{00} + (c_1^+ c_2^- - c_1^- c_2^+) A_{i-1,j\pm 1}^{20}\}], \quad (23)
\end{aligned}$$

where  $c_1^\pm$  and  $c_2^\pm$  are given in Eqs. (14). The expressions for  $Us_{1,i+1,j}^+ S_{i,j}^- U^+ \mathcal{P}_0$ ,  $Us_{2,i-1,j}^+ S_{i,j}^- U^+ \mathcal{P}_0$ ,  $Us_{1,i+1,j}^- S_{i,j}^+ U^+ \mathcal{P}_0$ ,  $Us_{2,i-1,j}^- S_{i,j}^+ U^+ \mathcal{P}_0$  can be recovered from the equations (22)-(23) by interchanging the indices.

The expressions (22)-(23) can be subsequently inserted into Eq. (21) in order to get the effective Hamiltonian in the second order. However, this is rather cumbersome combinatorial problem and we provide here only a sketch of such calculation. At first let us consider the

diagonal terms, which appear by contracting the perturbation terms acting on the same sites:

$$\begin{aligned}
H^{(2)} = & \frac{(J'_{xy})^2}{4} \sum'_{i,j=1}^N \sum_{m \neq 0} \left( \frac{\mathcal{P}_0 U s_{1,i,j+1}^- S_{i,j}^+ U^+ \mathcal{P}_m U s_{1,i,j+1}^+ S_{i,j}^- U^+ \mathcal{P}_0}{E_0^{(0)} - E_m^{(0)}} \right. \\
& + \frac{\mathcal{P}_0 U s_{1,i,j+1}^+ S_{i,j}^- U^+ \mathcal{P}_m U s_{1,i,j+1}^- S_{i,j}^+ U^+ \mathcal{P}_0}{E_0^{(0)} - E_m^{(0)}} + \frac{\mathcal{P}_0 U s_{2,i,j-1}^- S_{i,j}^+ U^+ \mathcal{P}_m U s_{2,i,j-1}^+ S_{i,j}^- U^+ \mathcal{P}_0}{E_0^{(0)} - E_m^{(0)}} \\
& \left. + \frac{\mathcal{P}_0 U s_{2,i,j-1}^+ S_{i,j}^- U^+ \mathcal{P}_m U s_{2,i,j-1}^- S_{i,j}^+ U^+ \mathcal{P}_0}{E_0^{(0)} - E_m^{(0)}} \right) \\
& + \frac{(J'_{xy})^2}{4} \sum''_{i,j=1}^N \sum_{m \neq 0} \left( \frac{\mathcal{P}_0 U s_{1,i+1,j}^- S_{i,j}^+ U^+ \mathcal{P}_m U s_{1,i+1,j}^+ S_{i,j}^- U^+ \mathcal{P}_0}{E_0^{(0)} - E_m^{(0)}} \right. \\
& + \frac{\mathcal{P}_0 U s_{1,i+1,j}^+ S_{i,j}^- U^+ \mathcal{P}_m U s_{1,i+1,j}^- S_{i,j}^+ U^+ \mathcal{P}_0}{E_0^{(0)} - E_m^{(0)}} + \frac{\mathcal{P}_0 U s_{2,i-1,j}^- S_{i,j}^+ U^+ \mathcal{P}_m U s_{2,i-1,j}^+ S_{i,j}^- U^+ \mathcal{P}_0}{E_0^{(0)} - E_m^{(0)}} \\
& \left. + \frac{\mathcal{P}_0 U s_{2,i-1,j}^+ S_{i,j}^- U^+ \mathcal{P}_m U s_{2,i-1,j}^- S_{i,j}^+ U^+ \mathcal{P}_0}{E_0^{(0)} - E_m^{(0)}} \right), \tag{24}
\end{aligned}$$

where  $E_0^{(0)}$  is the energy of the singlet-dimer state, and  $E_m^{(0)}$  are the energies of the states excited by the perturbation operator.

Further we will single out terms containing one, two or more triplet states separately. At first we extract the terms containing projection to the triplet excitation just on one site, while other sites are either in the singlet state or their states are not specified. It gives the one-particle contribution

$$\begin{aligned}
H_1^{(2)} &= E_0 \sum_{i,j} A_{i,j}^{11} \mathcal{P}_0, \\
E_0 &= -\frac{(J'_{xy})^2}{4} \left\{ 2 \left[ \frac{(c_1^+ + c_1^-)^2 (c_1^+)^6}{J} + 2 \frac{(c_1^+ + c_1^-)^2 (c_1^+)^4 (c_1^-)^2}{J + \sqrt{J^2 + J'^2}} + \frac{(c_1^+ + c_1^-)^2 (c_1^+)^4 (c_1^-)^2}{2J} \right] \right. \\
& \left. + 4 \left( \frac{(c_1^+)^6 (c_1^-)^2}{3J - J' - \sqrt{J^2 + J'^2}} + \frac{(c_1^+)^6 (c_1^-)^2}{3J - \sqrt{J^2 + J'^2}} \right) \right\}. \tag{25}
\end{aligned}$$

Hereafter we retain the contributions up to  $(c_1^-)^2$  ( $(c_1^+)^2 \approx 0.91$ ,  $(c_1^-)^2 \approx 0.09$  at the limiting value  $J'/J = 0.7$ ). The contribution for the two-triplon interaction can be found by extracting from Eq. (24) the terms containing the product of projections on two triplon states. Additionally, we have to subtract the one-particle contributions due to the relation  $A_{i,j}^{00} = 1 - A_{i,j}^{11}$ . As a result we get:

$$\begin{aligned}
H_2^{(2)} &= \left\{ \sum_{i,j} \left[ K_1 A_{i,j}^{11} \sum_{n_1=\pm 1} \sum_{n_2=\pm 1} A_{i+n_1,j+n_2}^{11} \right. \right. \\
& \left. + K_2 A_{i,j}^{11} \left( \sum_{n_1=\pm 2} \sum_{n_2=\pm 1} A_{i+n_1,j+n_2}^{11} + \sum_{n_1=\pm 1} \sum_{n_2=\pm 2} A_{i+n_1,j+n_2}^{11} \right) \right] \\
& \left. + K_3 \left( \sum'_{i,j=1}^N A_{i,j}^{11} \sum_{n_1=\pm 3} \sum_{n_2=\pm 1} A_{i+n_1,j+n_2}^{11} + \sum''_{i,j=1}^N A_{i,j}^{11} \sum_{n_1=\pm 1} \sum_{n_2=\pm 3} A_{i+n_1,j+n_2}^{11} \right) \right\} \mathcal{P}_0, \tag{26}
\end{aligned}$$

where the effective parameters are as follows:

$$\begin{aligned}
K_1 = & -\frac{(J'_{xy})^2}{4} \left[ \frac{2(c_1^+ + c_1^-)^2 (c_1^+)^4}{J + J' + \sqrt{J^2 + J'^2}} + \frac{2(c_1^+ + c_1^-)^2 (c_1^+)^2 (c_1^-)^2}{J + J' + 3\sqrt{J^2 + J'^2}} + \frac{2(c_1^+ + c_1^-)^2 (c_1^+)^2 (c_1^-)^2}{3J + J' + \sqrt{J^2 + J'^2}} \right. \\
& + \frac{2(c_1^+)^4 (c_1^-)^2}{5J - 3J' - \sqrt{J^2 + J'^2}} + \frac{(c_1^+)^6 (c_1^-)^2}{2J - J'} + \frac{2(c_1^+)^4 (c_1^-)^2}{5J + J' - \sqrt{J^2 + J'^2}} \\
& + \frac{2(c_1^+ + c_1^-)^2 (c_1^+)^6 (c_1^-)^2}{-J + J' + \sqrt{J^2 + J'^2}} + \frac{2(c_1^+ - c_1^-)^2 (c_1^+)^6 (c_1^-)^2}{-J + J' + 3\sqrt{J^2 + J'^2}} + \frac{2(c_1^+ c_2^+ + c_1^- c_2^-)^2 (c_1^+)^2 (c_1^-)^2}{5J - \sqrt{J^2 + 4J'^2}} \\
& - \frac{(c_1^+ + c_1^-)^2 (c_1^+)^6}{J} - 2 \frac{(c_1^+ + c_1^-)^2 (c_1^+)^4 (c_1^-)^2}{J + \sqrt{J^2 + J'^2}} - \frac{(c_1^+ + c_1^-)^2 (c_1^+)^4 (c_1^-)^2}{2J} \\
& \left. - 3 \left( \frac{(c_1^+)^6 (c_1^-)^2}{3J - J' - \sqrt{J^2 + J'^2}} + \frac{(c_1^+)^6 (c_1^-)^2}{3J - \sqrt{J^2 + J'^2}} \right) \right], \\
K_2 = & \frac{(J'_{xy})^2}{8} \left[ \frac{(c_1^+ + c_1^-)^2 (c_1^+)^6}{\sqrt{J^2 + J'^2}} + \frac{(c_1^+ + c_1^-)^2 (c_1^+)^4 (c_1^-)^2}{J + \sqrt{J^2 + J'^2}} + \frac{(c_1^+ + c_1^-)^2 (c_1^+)^4 (c_1^-)^2}{2\sqrt{J^2 + J'^2}} \right. \\
& + \frac{2(c_1^+)^4 (c_1^-)^2}{5J - J' - \sqrt{J^2 + J'^2}} + \frac{2(c_1^+ c_2^+ + c_1^- c_2^-)^2 (c_1^+)^4 (c_1^-)^2}{5J - 2J' - \sqrt{J^2 + 4J'^2}} + \frac{2(c_1^+ - c_1^-)^2 (c_1^+)^6 (c_1^-)^2}{5J - J' - \sqrt{J^2 + J'^2}} \\
& + \frac{2(c_1^+)^4 (c_1^-)^2}{5J - J' - \sqrt{J^2 + J'^2}} + \frac{(c_1^+)^6 (c_1^-)^2}{2J} + \frac{2(c_1^+ + c_1^-)^2 (c_1^+)^6 (c_1^-)^2}{5J - J' - \sqrt{J^2 + J'^2}} \\
& - \frac{(c_1^+ + c_1^-)^2 (c_1^+)^6}{J} - 2 \frac{(c_1^+ + c_1^-)^2 (c_1^+)^4 (c_1^-)^2}{J + \sqrt{J^2 + J'^2}} - \frac{(c_1^+ + c_1^-)^2 (c_1^+)^4 (c_1^-)^2}{2J} \\
& \left. - 3 \left( \frac{(c_1^+)^6 (c_1^-)^2}{3J - J' - \sqrt{J^2 + J'^2}} + \frac{(c_1^+)^6 (c_1^-)^2}{3J - \sqrt{J^2 + J'^2}} \right) \right], \\
K_3 = & \frac{(J'_{xy})^2}{4} \left[ \frac{(c_1^+)^6 (c_1^-)^2}{2J - J'} + \frac{2(c_1^+ c_2^+ + c_1^- c_2^-)^2 (c_1^+)^4 (c_1^-)^2}{5J - \sqrt{J^2 + 4J'^2}} - \frac{(c_1^+)^6 (c_1^-)^2}{3J - J' - \sqrt{J^2 + J'^2}} \right. \\
& \left. - \frac{(c_1^+)^6 (c_1^-)^2}{3J - \sqrt{J^2 + J'^2}} \right]. \tag{27}
\end{aligned}$$

The significant part of three-particle interactions includes the triplon configurations where at least two of them are at the closest location with respect to each other. It corresponds to the

following effective Hamiltonian:

$$\begin{aligned}
H_3^{(2)} = & \left\{ K_{\Delta 1} \left( \sum_{i,j=1}^N A_{i,j}^{11} \sum_{n=\pm 1} A_{i-1,j+n}^{11} A_{i+1,j+n}^{11} + \sum_{i,j=1}^N A_{i,j}^{11} \sum_{n=\pm 1} A_{i+n,j-1}^{11} A_{i+n,j+1}^{11} \right) \right. \\
& + K'_{\Delta 1} \sum_{i,j=1}^N A_{i,j}^{11} (A_{i-1,j-1}^{11} A_{i+1,j+1}^{11} + A_{i-1,j+1}^{11} A_{i+1,j-1}^{11}) \\
& + K_{\Delta 2} \left[ \sum_{i,j=1}^N A_{i,j}^{11} \sum_{n=\pm 1} (A_{i-1,j+n}^{11} A_{i+2,j+n}^{11} + A_{i-2,j+n}^{11} A_{i+1,j+n}^{11}) \right. \\
& + \left. \sum_{i,j=1}^N A_{i,j}^{11} \sum_{n=\pm 1} (A_{i+n,j-1}^{11} A_{i+n,j+2}^{11} + A_{i+n,j-2}^{11} A_{i+n,j+1}^{11}) \right] \\
& + K'_{\Delta 2} \sum_{i,j=1}^N A_{i,j}^{11} \sum_{n=\pm 1} (A_{i-2n,j-n}^{11} A_{i-n,j-2n}^{11} + A_{i+2n,j-n}^{11} A_{i+n,j-2n}^{11}) \\
& + K''_{\Delta 2} \left[ \sum_{i,j=1}^N A_{i,j}^{11} \sum_{n=\pm 1} (A_{i-2n,j-n}^{11} A_{i-3n,j}^{11} + A_{i+2n,j-n}^{11} A_{i+3n,j}^{11}) \right. \\
& + \left. \sum_{i,j=1}^N A_{i,j}^{11} \sum_{n=\pm 1} (A_{i-n,j-2n}^{11} A_{i,j-3n}^{11} + A_{i-n,j+2n}^{11} A_{i,j+3n}^{11}) \right] \\
& \left. + K_{\Delta 3} \left[ \sum_{i,j=1}^N A_{i,j}^{11} \sum_{n=\pm 1} A_{i-2,j+n}^{11} A_{i+2,j+n}^{11} + \sum_{i,j=1}^N A_{i,j}^{11} \sum_{n=\pm 1} A_{i+n,j-2}^{11} A_{i+n,j+2}^{11} \right] \right\} \mathcal{P}_0. \quad (28)
\end{aligned}$$

We omit here the explicit expressions for the effective three-particle couplings because of their extensive length. However, the dependencies of these parameters are shown in Fig. 6(b).

The contribution of quantum terms is obtained by contracting the terms corresponding

to neighboring interdimer couplings:

$$\begin{aligned}
H^{(2)} = & \frac{(J'_{xy})^2}{4} \sum_{i,j=1}^N \sum_{m \neq 0} \left( \frac{\mathcal{P}_0 U s_{2,i,j-1}^- S_{i,j}^+ U^+ \mathcal{P}_m U s_{1,i,j+1}^+ S_{i,j}^- U^+ \mathcal{P}_0}{E_0^{(0)} - E_m^{(0)}} \right. \\
& + \frac{\mathcal{P}_0 U s_{2,i,j-1}^+ S_{i,j}^- U^+ \mathcal{P}_m U s_{1,i,j+1}^- S_{i,j}^+ U^+ \mathcal{P}_0}{E_0^{(0)} - E_m^{(0)}} + \frac{\mathcal{P}_0 U s_{1,i,j+1}^- S_{i,j}^+ U^+ \mathcal{P}_m U s_{2,i,j-1}^+ S_{i,j}^- U^+ \mathcal{P}_0}{E_0^{(0)} - E_m^{(0)}} \\
& \left. + \frac{\mathcal{P}_0 U s_{1,i,j+1}^+ S_{i,j}^- U^+ \mathcal{P}_m U s_{2,i,j-1}^- S_{i,j}^+ U^+ \mathcal{P}_0}{E_0^{(0)} - E_m^{(0)}} \right) \\
& + \frac{(J'_{xy})^2}{4} \sum_{i,j=1}^N \sum_{m \neq 0} \left( \frac{\mathcal{P}_0 U s_{2,i-1,j}^- S_{i,j}^+ U^+ \mathcal{P}_m U s_{1,i+1,j}^+ S_{i,j}^- U^+ \mathcal{P}_0}{E_0^{(0)} - E_m^{(0)}} \right. \\
& + \frac{\mathcal{P}_0 U s_{2,i-1,j}^+ S_{i,j}^- U^+ \mathcal{P}_m U s_{1,i+1,j}^- S_{i,j}^+ U^+ \mathcal{P}_0}{E_0^{(0)} - E_m^{(0)}} + \frac{\mathcal{P}_0 U s_{1,i+1,j}^- S_{i,j}^+ U^+ \mathcal{P}_m U s_{2,i-1,j}^+ S_{i,j}^- U^+ \mathcal{P}_0}{E_0^{(0)} - E_m^{(0)}} \\
& \left. + \frac{\mathcal{P}_0 U s_{1,i+1,j}^+ S_{i,j}^- U^+ \mathcal{P}_m U s_{2,i-1,j}^- S_{i,j}^+ U^+ \mathcal{P}_0}{E_0^{(0)} - E_m^{(0)}} \right). \tag{29}
\end{aligned}$$

Eq. (29) can be recast into the form involving the correlated hopping of triplet excitations on a lattice:

$$\begin{aligned}
H_t^{(2)} = & \sum_{i,j=1}^N t (A_{i,j-1}^{11} + A_{i,j+1}^{11}) (A_{i+1,j}^{10} A_{i-1,j}^{01} + A_{i+1,j}^{01} A_{i-1,j}^{10}) \\
& + \sum_{i,j=1}^N t (A_{i-1,j}^{11} + A_{i+1,j}^{11}) (A_{i,j+1}^{10} A_{i,j-1}^{01} + A_{i,j+1}^{01} A_{i,j-1}^{10}) \\
t = & \frac{(J'_{xy})^2}{4} (c_1^+)^4 (c_1^-)^2 \left[ \frac{2}{5J - 3J' - \sqrt{J^2 + J'^2}} + \frac{2(c_1^+ + c_1^-)^2 (c_1^+)^2}{-J + J' + \sqrt{J^2 + J'^2}} \right]. \tag{30}
\end{aligned}$$

All second-order contributions given by Eqs. (25)-(29) are collected in the effective Hamiltonian:

$$H_{eff}^{(2)} = H_0^{(2)} + H_1^{(2)} + H_t^{(2)} + H_2^{(2)} + H_3^{(2)} + \dots \tag{31}$$

Instead of the projection operators we can introduce the representation of the quantum lattice gas, where  $n_{i,j} = A_{i,j}^{11}$  is the occupation number operator, and  $a_{i,j}^+ = A_{i,j}^{10}$  ( $a_{i,j} = A_{i,j}^{01}$ ) is the triplon creation (annihilation) operator. Thus, the effective Hamiltonian can be presented in



a more compact form:

$$\begin{aligned}
H_1^{(2)} &= E_0 \sum_{\mathbf{l}} n_{\mathbf{l}}, \\
H_2^{(2)} &= V_1 \sum_{\langle \mathbf{l}, \mathbf{l}' \rangle} n_{\mathbf{l}} n_{\mathbf{l}'} + V_2 \sum_{\langle \mathbf{l}, \mathbf{l}' \rangle'} n_{\mathbf{l}} n_{\mathbf{l}'} + V_3 \sum_{\langle \mathbf{l}, \mathbf{l}' \rangle''} n_{\mathbf{l}} n_{\mathbf{l}'}, \\
H_3^{(2)} &= V_{\Delta 1} \sum_{\langle \mathbf{l}, \mathbf{l}', \mathbf{l}'' \rangle_1} n_{\mathbf{l}} n_{\mathbf{l}'} n_{\mathbf{l}''} + V'_{\Delta 1} \sum_{\langle \mathbf{l}, \mathbf{l}', \mathbf{l}'' \rangle_1} n_{\mathbf{l}} n_{\mathbf{l}'} n_{\mathbf{l}''} + V_{\Delta 2} \sum_{\langle \mathbf{l}, \mathbf{l}', \mathbf{l}'' \rangle_2} n_{\mathbf{l}} n_{\mathbf{l}'} n_{\mathbf{l}''} \\
&\quad + V'_{\Delta 2} \sum_{\langle \mathbf{l}, \mathbf{l}', \mathbf{l}'' \rangle'_2} n_{\mathbf{l}} n_{\mathbf{l}'} n_{\mathbf{l}''} + V''_{\Delta 2} \sum_{\langle \mathbf{l}, \mathbf{l}', \mathbf{l}'' \rangle''_2} n_{\mathbf{l}} n_{\mathbf{l}'} n_{\mathbf{l}''} + V_{\Delta 3} \sum_{\langle \mathbf{l}, \mathbf{l}', \mathbf{l}'' \rangle'_3} n_{\mathbf{l}} n_{\mathbf{l}'} n_{\mathbf{l}''}, \\
H_t^{(2)} &= \sum_{i,j=1}^N t(n_{i,j-1} + n_{i,j+1})(a_{i+1,j}^+ a_{i-1,j} + a_{i+1,j} a_{i-1,j}^+) \\
&\quad + \sum_{i,j=1}^N t(n_{i-1,j} + n_{i+1,j})(a_{i,j+1}^+ a_{i,j-1} + a_{i,j+1} a_{i,j-1}^+),
\end{aligned} \tag{32}$$

where  $V_1 = 2K_1$ ,  $V_2 = 2K_2$ ,  $V_3 = 2K_3$ ,  $V_{\Delta 1} = K_{\Delta 1}$ ,  $V'_{\Delta 1} = K'_{\Delta 1}$ ,  $V''_{\Delta 1} = K''_{\Delta 1}$ ,  $V_{\Delta 3} = K_{\Delta 3}$ ,  $V_{\Delta 4} = K_{\Delta 4}$ .

## References

- [1] B. Sriram Shastry and B. Sutherland, *Exact ground state of a quantum mechanical antiferromagnet*, Physica B+C **108**(1), 1069 (1981), doi:10.1016/0378-4363(81)90838-X.
- [2] S. Miyahara and K. Ueda, *Theory of the orthogonal dimer Heisenberg spin model for  $SrCu_2(BO_3)_2$* , Journal of Physics: Condensed Matter **15**(9), R327 (2003), doi:10.1088/0953-8984/15/9/201.
- [3] A. Koga and N. Kawakami, *Quantum Phase Transitions in the Shastry-Sutherland Model for  $SrCu_2(BO_3)_2$* , Phys. Rev. Lett. **84**, 4461 (2000), doi:10.1103/PhysRevLett.84.4461.
- [4] M. Takigawa and F. Mila, *Magnetization Plateaux*, pp. 241–267, Springer Berlin Heidelberg, Berlin, Heidelberg, ISBN 978-3-642-10589-0, doi:10.1007/978-3-642-10589-0\_10 (2011).
- [5] A. Abendschein and S. Capponi, *Effective Theory of Magnetization Plateaux in the Shastry-Sutherland Lattice*, Phys. Rev. Lett. **101**, 227201 (2008), doi:10.1103/PhysRevLett.101.227201.
- [6] J. Dorier, K. P. Schmidt and F. Mila, *Theory of Magnetization Plateaux in the Shastry-Sutherland Model*, Phys. Rev. Lett. **101**, 250402 (2008), doi:10.1103/PhysRevLett.101.250402.
- [7] M. Nemeč, G. R. Foltin and K. P. Schmidt, *Microscopic mechanism for the  $\frac{1}{8}$  magnetization plateau in  $SrCu_2(BO_3)_2$* , Phys. Rev. B **86**, 174425 (2012), doi:10.1103/PhysRevB.86.174425.

- [8] G. R. Foltin, S. R. Manmana and K. P. Schmidt, *Exotic magnetization plateaus in a quasi-two-dimensional Shastry-Sutherland model*, Phys. Rev. B **90**, 104404 (2014), doi:10.1103/PhysRevB.90.104404.
- [9] P. Corboz and F. Mila, *Crystals of Bound States in the Magnetization Plateaus of the Shastry-Sutherland Model*, Phys. Rev. Lett. **112**, 147203 (2014), doi:10.1103/PhysRevLett.112.147203.
- [10] Y. H. Matsuda, N. Abe, S. Takeyama, H. Kageyama, P. Corboz, A. Honecker, S. R. Manmana, G. R. Foltin, K. P. Schmidt and F. Mila, *Magnetization of  $SrCu_2(BO_3)_2$  in Ultrahigh Magnetic Fields up to 118 T*, Phys. Rev. Lett. **111**, 137204 (2013), doi:10.1103/PhysRevLett.111.137204.
- [11] P. Corboz and F. Mila, *Tensor network study of the Shastry-Sutherland model in zero magnetic field*, Phys. Rev. B **87**, 115144 (2013), doi:10.1103/PhysRevB.87.115144.
- [12] H. Kageyama, M. Nishi, N. Aso, K. Onizuka, T. Yosihama, K. Nukui, K. Kodama, K. Kakurai and Y. Ueda, *Direct Evidence for the Localized Single-Triplet Excitations and the Dispersive Multitriplet Excitations in  $SrCu_2(BO_3)_2$* , Phys. Rev. Lett. **84**, 5876 (2000), doi:10.1103/PhysRevLett.84.5876.
- [13] C. Knetter, A. Bühler, E. Müller-Hartmann and G. S. Uhrig, *Dispersion and Symmetry of Bound States in the Shastry-Sutherland Model*, Phys. Rev. Lett. **85**, 3958 (2000), doi:10.1103/PhysRevLett.85.3958.
- [14] T. Momoi and K. Totsuka, *Magnetization plateaus of the Shastry-Sutherland model for  $SrCu_2(BO_3)_2$ : Spin-density wave, supersolid, and bound states*, Phys. Rev. B **62**, 15067 (2000), doi:10.1103/PhysRevB.62.15067.
- [15] K. Totsuka, S. Miyahara and K. Ueda, *Low-Lying Magnetic Excitation of the Shastry-Sutherland Model*, Phys. Rev. Lett. **86**, 520 (2001), doi:10.1103/PhysRevLett.86.520.
- [16] Y. Fukumoto, *Two-Triplet-Dimer Excitation Spectra in the Shastry-Sutherland Model for  $SrCu_2(BO_3)_2$* , Journal of the Physical Society of Japan **69**(9), 2755 (2000), doi:10.1143/JPSJ.69.2755, <https://doi.org/10.1143/JPSJ.69.2755>.
- [17] P. A. McClarty, F. Krüger, T. Guidi, S. F. Parker, K. Refson, A. W. Parker, D. Prabhakaran and R. Coldea, *Topological triplon modes and bound states in a Shastry-Sutherland magnet*, Nature Physics **13**(8), 736 (2017), doi:10.1038/nphys4117, 1609.01922.
- [18] M. Malki and K. P. Schmidt, *Magnetic Chern bands and triplon Hall effect in an extended Shastry-Sutherland model*, Phys. Rev. B **95**, 195137 (2017), doi:10.1103/PhysRevB.95.195137.
- [19] F. Levy, I. Sheikin, C. Berthier, M. Horvatić, M. Takigawa, H. Kageyama, T. Waki and Y. Ueda, *Field dependence of the quantum ground state in the Shastry-Sutherland system  $SrCu_2(BO_3)_2$* , EPL (Europhysics Letters) **81**(6), 67004 (2008), doi:10.1209/0295-5075/81/67004.
- [20] Z. Wang and C. D. Batista, *Dynamics and Instabilities of the Shastry-Sutherland Model*, Phys. Rev. Lett. **120**, 247201 (2018), doi:10.1103/PhysRevLett.120.247201.

- [21] S. Wessel, I. Niesen, J. Stapmanns, B. Normand, F. Mila, P. Corboz and A. Honecker, *Thermodynamic properties of the Shastry-Sutherland model from quantum Monte Carlo simulations*, Phys. Rev. B **98**, 174432 (2018), doi:10.1103/PhysRevB.98.174432.
- [22] A. Wietek, P. Corboz, S. Wessel, B. Normand, F. Mila and A. Honecker, *Thermodynamic properties of the Shastry-Sutherland model throughout the dimer-product phase*, Phys. Rev. Research **1**, 033038 (2019), doi:10.1103/PhysRevResearch.1.033038.
- [23] H. Tsujii, C. R. Rotundu, B. Andraka, Y. Takano, H. Kageyama and Y. Ueda, *Specific Heat of the  $S=1/2$  Two-Dimensional Shastry-Sutherland Antiferromagnet  $SrCu_2(BO_3)_2$  in High Magnetic Fields*, Journal of the Physical Society of Japan **80**(4), 043707 (2011), doi:10.1143/JPSJ.80.043707, <https://doi.org/10.1143/JPSJ.80.043707>.
- [24] Y. Sassa, S. Wang, J. Sugiyama, A. Amato, H. M. Rønnow, C. Rüegg and M. Månsson,  *$\mu^+SR$  Investigation of the Shastry-Sutherland Compound  $SrCu_2(BO_3)_2$* , In *Proceedings of the 14th International Conference on Muon Spin Rotation*, p. 011010, doi:10.7566/JPSCP.21.011010 (2018).
- [25] P. Czarnik, M. M. Rams, P. Corboz and J. Dziarmaga, *Tensor network study of the  $m = \frac{1}{2}$  magnetization plateau in the Shastry-Sutherland model at finite temperature*, Phys. Rev. B **103**, 075113 (2021), doi:10.1103/PhysRevB.103.075113.
- [26] H. Kageyama, K. Yoshimura, R. Stern, N. V. Mushnikov, K. Onizuka, M. Kato, K. Kosuge, C. P. Slichter, T. Goto and Y. Ueda, *Exact Dimer Ground State and Quantized Magnetization Plateaus in the Two-Dimensional Spin System  $SrCu_2(BO_3)_2$* , Phys. Rev. Lett. **82**, 3168 (1999), doi:10.1103/PhysRevLett.82.3168.
- [27] M. Takigawa, M. Horvatić, T. Waki, S. Krämer, C. Berthier, F. Lévy-Bertrand, I. Sheikin, H. Kageyama, Y. Ueda and F. Mila, *Incomplete Devil's Staircase in the Magnetization Curve of  $SrCu_2(BO_3)_2$* , Phys. Rev. Lett. **110**, 067210 (2013), doi:10.1103/PhysRevLett.110.067210.
- [28] M. E. Zayed, C. Rüegg, J. Larrea J., A. M. Läuchli, C. Panagopoulos, S. S. Saxena, M. Ellerby, D. F. McMorrow, T. Strässle, S. Klotz, G. Hamel, R. A. Sadykov *et al.*, *4-spin plaquette singlet state in the Shastry-Sutherland compound  $SrCu_2(BO_3)_2$* , Nature Physics **13**(10), 962 (2017), doi:10.1038/nphys4190, 1603.02039.
- [29] T. Sakurai, Y. Hirao, K. Hijii, S. Okubo, H. Ohta, Y. Uwatoko, K. Kudo and Y. Koike, *Direct Observation of the Quantum Phase Transition of  $SrCu_2(BO_3)_2$  by High-Pressure and Terahertz Electron Spin Resonance*, Journal of the Physical Society of Japan **87**(3), 033701 (2018), doi:10.7566/JPSJ.87.033701, <https://doi.org/10.7566/JPSJ.87.033701>.
- [30] C. Boos, S. P. G. Crone, I. A. Niesen, P. Corboz, K. P. Schmidt and F. Mila, *Competition between intermediate plaquette phases in  $SrCu_2(BO_3)_2$  under pressure*, Phys. Rev. B **100**, 140413 (2019), doi:10.1103/PhysRevB.100.140413.
- [31] D. I. Badrtdinov, A. A. Tsirlin, V. V. Mazurenko and F. Mila,  *$SrCu_2(BO_3)_2$  under pressure: A first-principles study*, Phys. Rev. B **101**, 224424 (2020), doi:10.1103/PhysRevB.101.224424.

- [32] J. Guo, G. Sun, B. Zhao, L. Wang, W. Hong, V. A. Sidorov, N. Ma, Q. Wu, S. Li, Z. Y. Meng, A. W. Sandvik and L. Sun, *Quantum Phases of  $SrCu_2(BO_3)_2$  from High-Pressure Thermodynamics*, Phys. Rev. Lett. **124**, 206602 (2020), doi:10.1103/PhysRevLett.124.206602.
- [33] S. Bettler, L. Stoppel, Z. Yan, S. Gvasaliya and A. Zheludev, *Sign switching of dimer correlations in  $SrCu_2(BO_3)_2$  under hydrostatic pressure*, Phys. Rev. Research **2**, 012010 (2020), doi:10.1103/PhysRevResearch.2.012010.
- [34] T. A. Kodenkandath, A. S. Kumbhar, W. L. Zhou and J. B. Wiley, *Construction of Copper Halide Networks within Layered Perovskites. Syntheses and Characterization of New Low-Temperature Copper Oxyhalides*, Inorg Chem. **40**(4), 710 (2001), doi:10.1021/ic0008215, <https://pubs.acs.org/doi/abs/10.1021/ic0008215>.
- [35] Y. Tsujimoto, A. Kitada, M. Nishi, Y. Narumi, K. Kindo, T. Goko, Y. J. Uemura, A. A. Aczel, T. J. Williams, G. M. Luke, Y. Ajiro and H. Kageyama, *Spin-Singlet Ground State of Two-Dimensional Quantum Spin Antiferromagnet  $(CuCl)Ca_2Nb_3O_{10}$* , Journal of the Physical Society of Japan **83**(7), 074712 (2014), doi:10.7566/JPSJ.83.074712, <https://doi.org/10.7566/JPSJ.83.074712>.
- [36] S. Yoshii, T. Yamamoto, M. Hagiwara, A. Shigekawa, S. Michimura, F. Iga, T. Takabatake and K. Kindo, *High-field magnetization of  $TmB_4$* , Journal of Physics: Conference Series **51**, 59 (2006), doi:10.1088/1742-6596/51/1/011.
- [37] S. Yoshii, T. Yamamoto, M. Hagiwara, S. Michimura, A. Shigekawa, F. Iga, T. Takabatake and K. Kindo, *Multistep Magnetization Plateaus in the Shastry-Sutherland System  $TbB_4$* , Phys. Rev. Lett. **101**, 087202 (2008), doi:10.1103/PhysRevLett.101.087202.
- [38] K. Siemensmeyer, E. Wulf, H.-J. Mikeska, K. Flachbart, S. Gabáni, S. Mat'aš, P. Priputen, A. Efdokimova and N. Shitsevalova, *Fractional Magnetization Plateaus and Magnetic Order in the Shastry-Sutherland Magnet  $TmB_4$* , Phys. Rev. Lett. **101**, 177201 (2008), doi:10.1103/PhysRevLett.101.177201.
- [39] T. Matsumura, D. Okuyama, T. Mouri and Y. Murakami, *Successive Magnetic Phase Transitions of Component Orderings in  $DyB_4$* , Journal of the Physical Society of Japan **80**(7), 074701 (2011), doi:10.1143/JPSJ.80.074701, <https://doi.org/10.1143/JPSJ.80.074701>.
- [40] J. Trinh, S. Mitra, C. Panagopoulos, T. Kong, P. C. Canfield and A. P. Ramirez, *Degeneracy of the  $1/8$  Plateau and Antiferromagnetic Phases in the Shastry-Sutherland Magnet  $TmB_4$* , Phys. Rev. Lett. **121**, 167203 (2018), doi:10.1103/PhysRevLett.121.167203.
- [41] S. Gabáni, I. Takáčová, M. Orendáč, G. Pristáš, E. Gažo, K. Siemensmeyer, A. Bogach, N. Sluchanko, N. Shitsevalova, J. Prokleška, V. Sechovský and K. Flachbart, *Spin, charge and lattice dynamics of magnetization processes in frustrated shastry-sutherland system  $tmb_4$* , Solid State Sciences **105**, 106210 (2020), doi:<https://doi.org/10.1016/j.solidstatesciences.2020.106210>.
- [42] M. Orendáč, S. Gabáni, P. Farkašovský, E. Gažo, J. Kačmarčík, M. Marcin, G. Pristáš, K. Siemensmeyer, N. Shitsevalova and K. Flachbart, *Ground state and stability of the*

- fractional plateau phase in metallic Shastry–Sutherland system  $TmB_4$* , Scientific Reports **11**, 6835 (2021), doi:10.1038/s41598-021-86353-5.
- [43] Y. I. Dublenych, *Ground states of the ising model on the shastry-sutherland lattice and the origin of the fractional magnetization plateaus in rare-earth-metal tetraborides*, Phys. Rev. Lett. **109**, 167202 (2012), doi:10.1103/PhysRevLett.109.167202.
- [44] P. Farkašovský, H. Čenčariková and S. Mat’áš, *Numerical study of magnetization processes in rare-earth tetraborides*, Phys. Rev. B **82**, 054409 (2010), doi:10.1103/PhysRevB.82.054409.
- [45] P. Farkašovský and H. Čenčariková, *Phase Transitions in a Coupled Electron and Spin Model on the Shastry-Sutherland Lattice*, Acta Phys. Polonica A **126**, 44 (2014), doi:10.12693/APhysPolA.126.44.
- [46] F. Mila and K. P. Schmidt, *Strong-Coupling Expansion and Effective Hamiltonians*, pp. 537–559, Springer Berlin Heidelberg, Berlin, Heidelberg, ISBN 978-3-642-10589-0, doi:10.1007/978-3-642-10589-0\_20 (2011).
- [47] T. Verkholyak, J. Strečka, F. Mila and K. P. Schmidt, *Exact ground states of a spin- $\frac{1}{2}$  ising-heisenberg model on the shastry-sutherland lattice in a magnetic field*, Phys. Rev. B **90**, 134413 (2014), doi:10.1103/PhysRevB.90.134413.
- [48] K. P. Schmidt and G. S. Uhrig, *Excitations in one-dimensional  $s = \frac{1}{2}$  quantum antiferromagnets*, Phys. Rev. Lett. **90**, 227204 (2003), doi:10.1103/PhysRevLett.90.227204.
- [49] P. Fulde, *Electron Correlations in Molecules and Solids*, Springer Series in Solid-State Sciences. Springer Berlin Heidelberg, ISBN 978-3-540-59364-5, doi:10.1007/978-3-642-57809-0 (1995).
- [50] S. Miyahara and K. Ueda, *Exact Dimer Ground State of the Two Dimensional Heisenberg Spin System  $SrCu_2(BO_3)_2$* , Phys. Rev. Lett. **82**, 3701 (1999), doi:10.1103/PhysRevLett.82.3701.
- [51] M. Takigawa, T. Waki, M. Horvatić and C. Berthier, *Novel Ordered Phases in the Orthogonal Dimer Spin System  $SrCu_2(BO_3)_2$* , Journal of the Physical Society of Japan **79**(1), 011005 (2010), doi:10.1143/JPSJ.79.011005, <https://doi.org/10.1143/JPSJ.79.011005>.
- [52] S. Miyahara and K. Ueda, *Thermodynamic Properties of Three-Dimensional Orthogonal Dimer Model for  $SrCu_2(BO_3)_2$* , In *Proc. Int. Workshop on Magnetic Excitations in Strongly Correlated Electrons*, vol. 69, p. 72 (2000), <https://arxiv.org/abs/cond-mat/0004260>.
- [53] J. B. Parkinson, *Theory of spin waves in a one-dimensional Heisenberg antiferromagnet*, Journal of Physics C: Solid State Physics **12**(14), 2873 (1979), doi:10.1088/0022-3719/12/14/022.
- [54] Y. Xian, *A microscopic approach to the dimerization in frustrated spin-  $1/2$  antiferromagnetic chains*, Journal of Physics: Condensed Matter **6**(30), 5965 (1994), doi:10.1088/0953-8984/6/30/015.

- [55] T. Verkholyak and J. Strečka, *Fractional magnetization plateaus of the spin- $\frac{1}{2}$  heisenberg orthogonal-dimer chain: Strong-coupling approach developed from the exactly solved ising-heisenberg model*, Phys. Rev. B **94**, 144410 (2016), doi:10.1103/PhysRevB.94.144410.